

Original Article

Cite this article: Mirabella F, Braun T, Brogi A, and Capezzuoli E (2022) Pliocene–Quaternary seismogenic faults in the inner Northern Apennines (Valdelsa Basin, southern Tuscany) and their role in controlling the local seismicity. *Geological Magazine* **159**: 853–872. <https://doi.org/10.1017/S0016756822000036>

Received: 14 October 2021

Revised: 11 January 2022

Accepted: 13 January 2022

First published online: 10 February 2022




Keywords:

active faults; seismic profiles; earthquakes; strike-slip faults; inner Northern Apennines

Author for correspondence:

Francesco Mirabella,
Email: francesco.mirabella@unipg.it

Pliocene–Quaternary seismogenic faults in the inner Northern Apennines (Valdelsa Basin, southern Tuscany) and their role in controlling the local seismicity

Francesco Mirabella¹ , Thomas Braun², Andrea Brogi^{3,4}  and Enrico Capezzuoli⁵ 

¹Department of Physics and Geology, University of Perugia, 06123 Perugia, Italy; ²Istituto Nazionale di Geofisica e Vulcanologia, Sezione di Roma 1, Oss. di Arezzo, 52100 Arezzo, Italy; ³Department of Earth and Geoenvironmental Sciences, University of Bari, 70125 Bari, Italy; ⁴Institute of Geosciences and Earth Resources IGG-CNR, 56124 Pisa, Italy and ⁵Department of Earth Sciences, University of Florence, 50121 Florence, Italy

Abstract

Pliocene–Quaternary faults are relevant structures with which to constrain the seismotectonic context and contribute to the evaluation of the seismic hazard of a region. Many of these faults, however, do not show clear surface evidence even when releasing earthquakes. For these reasons they can be extremely dangerous as they receive relatively little attention and can be difficult to identify. From among the various surface geology studies and/or palaeoseismological investigations, we focus our attention on the integration of different datasets such as seismic reflection profiles, surface kinematic data and the relocation of seismological data, which make it possible to identify and characterize active faults whose dimension and earthquake potential would otherwise not be large enough to make them identifiable. We take as an example the Montespertoli NE-trending fault in southern Tuscany (central Italy) with which we associate the 2016 $M=3.9$ Castelfiorentino earthquake. This structure is part of a wider (in the order of 15–20 km) crustal-scale shear zone, which may be responsible for strong historical earthquakes in the area.

1. Introduction

Active faults capable of generating earthquakes may be blind, not reaching the ground surface, and/or be masked by continuous burial/erosion processes at the surface (e.g. Lettis *et al.* 1997).

Nevertheless, depending on their dimensions and depths, such structures may provide relevant surface or co-seismic effects, when activated. In some cases, faults can be capable of producing damaging earthquakes also generating surface primary ruptures. In some other cases, fault segments are too small to produce large-magnitude events and co-seismic surface effects, but are large enough to cause significant ground shaking and be clearly felt by the population. In both cases, these elusive faults represent structures that may prove very dangerous in populated areas, especially those with high vulnerability due to the presence of historic buildings. Several damaging earthquakes that have occurred in the recent past are interpreted as having been generated by blind faults (Whittier Narrows 1987 Los Angeles California (USA) $M=5.9$ – Hauksson *et al.* 1988; Haiti 2010 $M=7.0$ – Hayes *et al.* 2010; Christchurch 2010 New Zealand $M=7.1$ – Li *et al.* 2014; Van 2011 Turkey $M=7.1$ – Doğan & Karaka, 2013; Po Plain 2012 Italy $M=5.8$ – Burrato *et al.* 2012). In some cases, such faults never ruptured the surface but show signs of surface activity such as evidence of folding (e.g. Ventura anticline in California – Shaw & Suppe, 1994; Montello anticline in Italy – Benedetti *et al.* 2000). In many cases, no detailed information on the potential danger posed by such structures was given prior to the seismic events.

Other faults, though potentially active and seismogenic, are called ‘hidden’, their recent geological and morphological evidences being limited and hence difficult to identify or infer. For example, the $M=4.9$ earthquake in 2019 in France occurred on a reactivated Oligocene thrust fault with no geomorphic evidence of cumulative compressional deformation along the fault for several thousand or tens of thousands of years (Ritz *et al.* 2020). Such hidden structures can have important impacts on society because they are hard to find, for want of geological or morphological evidence. This implies the existence of active faults that have not yet been identified but that, at least in historical times, gave rise to considerable seismic events. These faults, not showing clear surface evidence of activity, remain mostly unidentified, most studies being focused on indirect surface evidence of their existence and activity.

In order to characterize the earthquake potential of these faults, different approaches are available which range from morphotectonic evidence to palaeoseismological investigations

(e.g. Hancock *et al.* 1999; Piccardi *et al.* 1999, 2017; Burrato *et al.* 2012; Brogi *et al.* 2017; Nirta *et al.* 2021).

Other approaches were also developed aiming at the integration of both surface and subsurface datasets including seismic interpretation, and borehole data, compared with seismological data to infer fault geometry and slip rates. In fact, the increasing availability of subsurface geological and geophysical information has afforded the opportunity to identify and map faults in the subsurface in great detail (e.g. Armijo *et al.* 1996; Pratt *et al.* 1998; Di Bucci *et al.* 2006; Mirabella *et al.* 2008; Bell *et al.* 2009; Toscani *et al.* 2009; Brogi *et al.* 2014). In some cases, comparison of geomorphic anomalies mapping with subsurface reconstructions results in effective identification of potentially active faults (e.g. Toscani *et al.* 2009 and references therein).

In this paper we focus on a fault system, active since the Neogene, affecting a sector of southern Tuscany (Valdelsa Basin, Fig. 1a). It generated low-magnitude earthquakes in 2014 and 2016 (Castelfiorentino and Certaldo earthquakes, $M = 3.9$ (25 October 2016) and $M = 3.4$ (9 August 2014) (Fig. 1b) in an area where the occurrence of active faults has never been documented before.

Notwithstanding the low magnitude of the events and the absence of important damage, these earthquakes occurred in an area where historically stronger events are documented (equivalent magnitude $M_e = 5.5$) and which has high vulnerability due to the presence of both high population density and historic and art-heritage buildings.

After an introduction to the geological and tectonic setting, we present a new interpretation of seismic reflection profiles, acquired for hydrocarbons exploration by the Agip oil company during the 1980s, and calibrated with borehole logs and surface fault kinematic data, and integrate them with an accurate relocation of the seismological data. We conclude that the Castelfiorentino and Certaldo earthquakes and their minor sequences are associated with a NE-trending fault system which belongs to a much wider crustal-scale structure, orthogonal to the main trend of the Valdelsa Basin. We discuss the role of these faults in controlling earthquakes, their detection by means of subsurface data and the possible correlation with geomorphological observations, and we frame their evolution in the Neogene–Quaternary tectonic setting of the inner Northern Apennines.

2. Geological and seismotectonic setting

The Northern Apennines originated from the convergence and collision (late Cretaceous – early Miocene) between the Adria promontory and the European plate, represented by the Sardinia–Corsica massif (Molli, 2008 and references therein). In the inner zone of the Northern Apennines this process gave rise to the stacking of several tectonic units derived from different palaeogeographic domains (Vai & Martini, 2001), namely, from top to bottom (Carmignani *et al.* 1994): (a) Ligurian units, derived from the Ligurian–Piedmont Domain, and consisting of remnants of Jurassic oceanic crust and its late Jurassic – Cretaceous, mainly clayey, sedimentary cover; (b) Sub-Ligurian units (Sub-Ligurian Domain), made up of Cretaceous–Oligocene turbidites; and (c) Tuscan units forming a duplex system and composed of high-pressure metamorphic and sedimentary units ranging from the Palaeozoic to the early Miocene (Pandeli *et al.* 1991; Carmignani *et al.* 1994; Rossetti *et al.* 2002; Brogi & Giorgetti, 2012; Bianco *et al.* 2015) (Fig. 2a). The Ligurian and Sub-Ligurian units were thrust eastward over the Tuscan Nappe during

the late Oligocene – early Miocene. After nappe stacking, eastward-migrating extension affected the inner Northern Apennines, i.e. northern Tyrrhenian Basin and Tuscany (e.g. Lavecchia, 1988; Patacca *et al.* 1990; Doglioni, 1991; Carmignani *et al.* 1994; Molli, 2008; Barchi, 2010; Rossetti *et al.* 2015) since the Miocene (Carmignani *et al.* 1994; Dallmeyer & Liotta, 1998; Liotta *et al.* 1998; Brogi & Liotta, 2008; Brogi, 2011) and determined the development of mainly eastward-dipping normal faults, which produced: (a) the lateral segmentation of the more competent levels within the previously stacked tectonic units (Decandia *et al.* 1993); (b) the consequent westward rotation of their hanging-walls (Brogi, 2004); (c) the direct superimposition of the Ligurian units on the late Triassic evaporite and/or on the Palaeozoic phyllites, both representing regional detachment levels (Brogi & Liotta, 2008); and (d) an extension of at least 120 % (Carmignani *et al.* 1994; Brogi, 2006). The youngest extensional event (Dallmeyer & Liotta, 1998; Barchi, 2010), active since the early Zanclean (Martini *et al.* 2021), is characterized by NW-trending normal faults cross-cutting the previously developed structures (Mazzanti, 1966; Calamai *et al.* 1970; Lazzarotto & Mazzanti, 1978) and defining tectonic depressions where Pliocene to Quaternary marine to continental sediments were deposited (Bossio *et al.* 1993a; Martini & Sagri, 1993). The amount of extension associated with this event is estimated in the order of 6–7 % (Carmignani *et al.* 1994). These depressions are coeval with NE-trending fault zones (Liotta, 1991) that controlled the volcanism and the emplacement of magmatic bodies at shallow crustal levels (Fig. 1a) (Acocella & Funicello, 2006; Dini *et al.* 2008; Brogi *et al.* 2010; Farina *et al.* 2010; Liotta *et al.* 2015). These SW–NE-trending fault zones (e.g. the Livorno–Sillaro line (Fig. 1b)), recognized by many authors since the 1960s through satellite image analyses (Ambrosetti *et al.* 1978; Boccaletti *et al.* 1985), are characterized by strike- to oblique-slip kinematics and associated horizontal displacements (see Basili & Valensise, 2001; Brogi *et al.* 2013; Liotta & Brogi, 2020). The origin and role of these structures is not well established, and they are variously interpreted as transfer zones, lateral ramps of thrusts and segmenting features of the NW–SE-trending extensional systems (Ghelardoni 1965; Boccaletti & Dainelli 1982; Fazzini & Gelmini 1982; Rosenbaum & Piana Agostinetti 2015). One of these main fault zones (referred to as the ‘Piombino–Faenza line’) crosses the study area (Fig. 1b) and interrupts the continuity of the Valdelsa Basin and of other basins (the Firenze (Florence), Casino -CSN and Volterra basins in Fig. 1b) (Canuti *et al.* 1966; Bossio *et al.* 2002).

The Neogene extensional setting and evolution, confirmed by many field and laboratory studies (among others, Lavecchia, 1988; Jolivet *et al.* 1990; Carmignani *et al.* 1994; Bartole, 1995; Barchi *et al.* 1998; Gualtieri *et al.* 1998; Liotta *et al.* 1998; Negrodo *et al.* 1999; Rossetti *et al.* 1999; Di Bucci & Mazzoli, 2002; Pera *et al.* 2003; Collettini *et al.* 2006; Brogi, 2008) has been challenged by alternative interpretations (e.g. Bonini & Moratti, 1995; Finetti *et al.* 2001; Bonini & Sani, 2002; Finetti, 2006; Bonini *et al.* 2014). A discussion of the reasons why an extensional setting better explains the regional geological features of Tuscany is provided in Brogi *et al.* (2005), Brogi & Liotta (2008) and Brogi (2011, 2020), to which we address the reader for further information.

The inner zone of the Northern Apennines is characterized by low-magnitude seismic events ($M < 4.5$) mainly confined to the shallow crust, at depths ranging between 3 and 10 km (Selvaggi & Amato, 1992; Cameli *et al.* 1993; Batini *et al.* 1985;

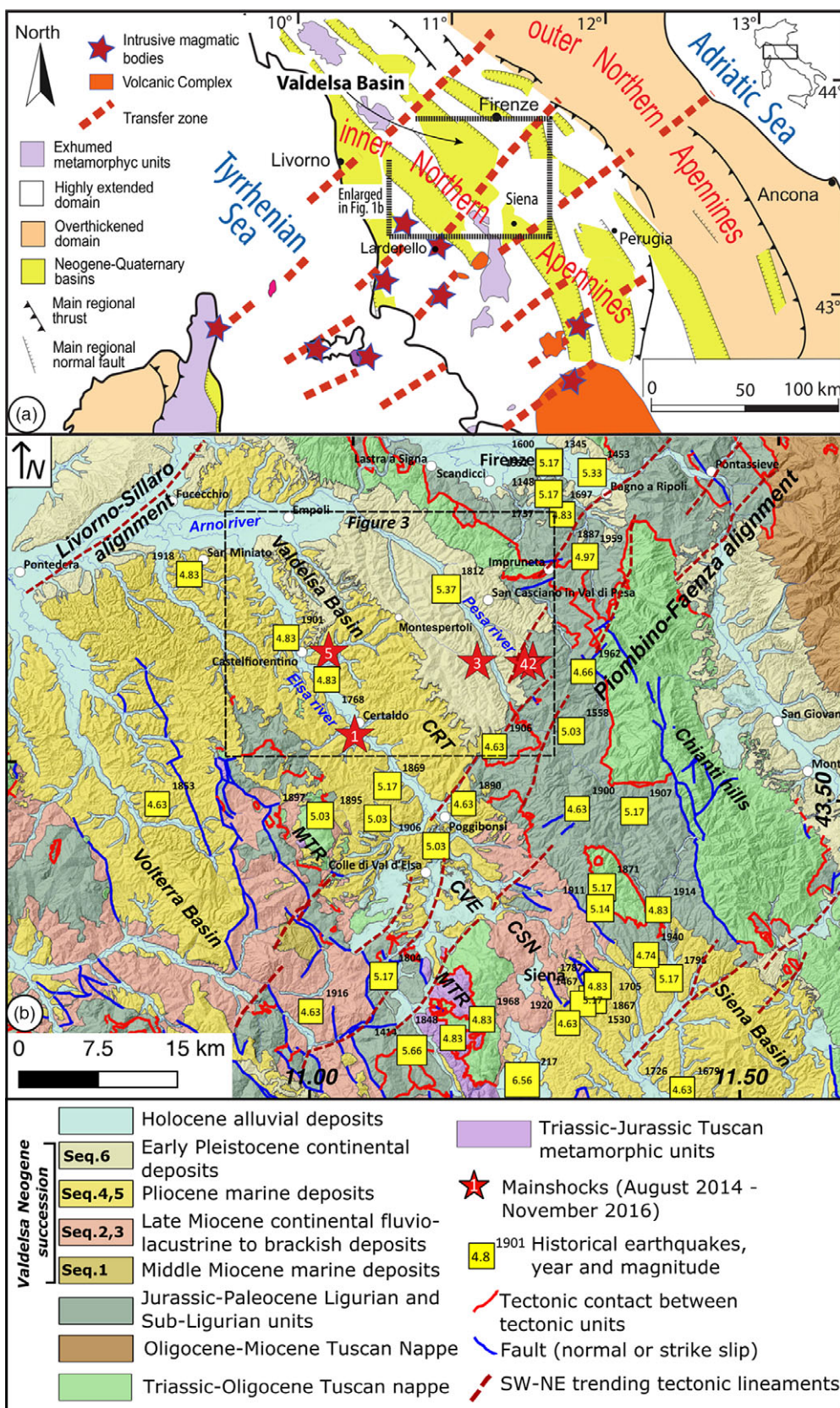


Fig. 1. (Colour online) (a) Tectonic sketch of the Inner Northern Apennines (Central Italy) showing the relationships between the SW-NE lineaments, the Neogene-Quaternary basins and the intrusive magmatic bodies. (b) Geological map of the Valdelsa Basin with the main SW-NE-trending lineaments, the historical seismicity (equivalent magnitude $M_e > 4.5$), and the 2014-16 mainshocks relocated and discussed in this work. Within the map, the Valdelsa Neogene deposits are numbered from Sequence 1 to Sequence 6 for further reference in the text. MTR: Middle Tuscan Ridge; CRT: Certaldo Sub-Basin; CVE: Colle Val d'Elsa Sub-Basin; CSN: Casino Basin.

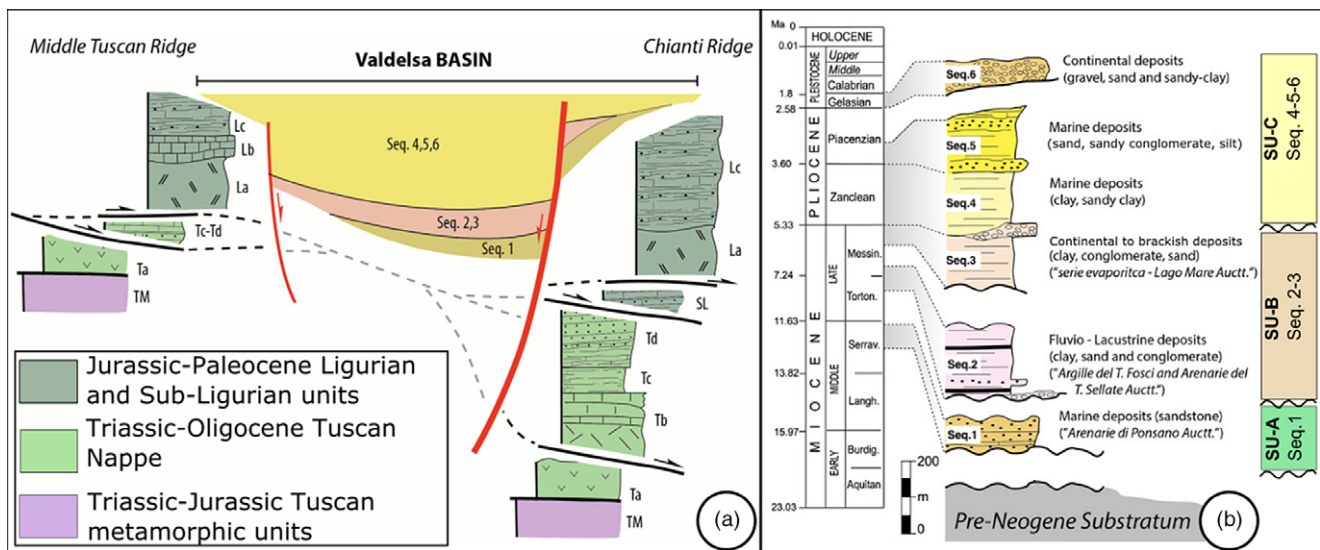


Fig. 2. (Colour online) (a) Sketch of the tectonic units of the inner Northern Apennines and of their relationship with the Valdelsa Basin infill. TM: Triassic Verrucano siliciclastics Group and Jurassic–Eocene metasedimentary cover; Ta: Late Triassic evaporite; Tc–Td: Cretaceous – early Miocene clayey and arenaceous succession; La: Jurassic oceanic crust (peridotites, gabbros and basalts); Lb: sedimentary cover made of Jurassic radiolarite and Cretaceous shale, clayey marl and limestone; Lc: S. Fiora unit composed of Cretaceous–Eocene clayey–marly and arenaceous succession. (b) Sequence-stratigraphic subdivision of the Neogene succession present in Valdelsa Basin and based on the distinctions proposed by Pascucci *et al.* (2007). Results composed by the superposition of marine (Seq. 1, 4, 5) and continental (Seq. 2, 3, 6) sequences characterized by variable thickness and lithological composition. To the right the sequences are grouped in relation to the seismic units (SU) shown later in the paper. Sequences are locally divided by unconformities (thicker undulated lines).

Di Bucci & Mazzoli, 2002; Braun *et al.* 2018a). The majority of earthquakes are concentrated in the geothermal areas of Tuscany, south of the study area (Larderello–Travale and Mount Amiata) and Northern Latium (Batini *et al.* 1985; Buonasorte *et al.* 1987; Cameli *et al.* 1993; Console & Rosini, 1998; Albarello *et al.* 2005; Braun *et al.* 2018a, b; Lisi *et al.* 2019), where some of them could probably be ascribed to the extraction and reinjection of geothermal fluids. Relatively low seismicity characterizes the other areas of Tuscany.

In terms of seismic hazard, southern Tuscany, as well as the inner Northern Apennines, was considered of modest interest and seismogenically less energetic, in contrast to outer zones (e.g. the Umbria–Marche and Abruzzo Regions and the Adriatic Sea), where earthquakes recorded in the last century reached magnitudes up to 6.8 (Avezzano earthquake, 1915; 32 000 victims (Console *et al.* 1993; De Luca *et al.* 1999; Galadini & Galli, 2000; Alessandrini *et al.* 2001; Chiarabba *et al.* 2005; Pace *et al.* 2006; Faenza & Pierdominici, 2007)).

Nevertheless, the available information on the historical seismicity of both the Valdelsa and Chianti areas in southern Tuscany (i.e. DBMI15, Locati *et al.* 2021) highlights a different scenario where damaging seismic events were documented (Boschi *et al.* 1997; Camassi *et al.* 2011) (Fig. 1b).

3. The Valdelsa Basin

The Valdelsa Basin (Fig. 3, location in Fig. 1b) is part of a broad Neogene NNW–SSE-oriented tectonic depression, crossing southern Tuscany from the Arno river (to the north) to the Bolsena lake (to the south) and comprehending the Siena and the Casino basins (Fig. 1b). The 70 km long Valdelsa Basin shows an articulated width, ranging from 30 km in its northern portion (Certaldo sub-basin) to less than 15 km in its southern sector (Colle Val d’Elsa sub-basin), with the threshold located in correspondence to a NE–SW-oriented tectonic lineament known as

the Piombino–Faenza line (Fig. 1b) (Ambrosetti *et al.* 1978; Boccaletti *et al.* 1985; Liotta, 1991).

The basin is delimited by the Middle-Tuscan Range and Chianti Hills to the SW and NE, respectively (Fig. 1b), where metamorphic and non-metamorphic units, forming the remnants of the Northern Apennines tectonic pile, are exposed. These units are, from the top (Fig. 2a): (a) the Ophiolitic Unit (the uppermost tectonic unit belonging to the Ligurian Complex) consisting of remnants of the Jurassic oceanic crust (serpentinized harzburgite, gabbro and basalt; La in Fig. 2a), and the sedimentary cover, mainly composed of Jurassic radiolarite and Cretaceous shale, clayey marl and limestone (Lb in Fig. 2a); (b) the S. Fiora Unit composed of Cretaceous–Eocene clayey–marly and arenaceous succession deposited on the oceanic crust of the Neo-Tethys (Lc in Fig. 2a); (c) the Canetolo Unit (Argille e calcari Auct.) composed of Eocene clayey–carbonate succession deposited in a transitional crustal sector passing from the oceanic crust to the Adria continental margin (SL in Fig. 2a); (d) the Tuscan Nappe representing the deepest non-metamorphic tectonic units of the Northern Apennines, composed of Late Triassic evaporite (Ta in Fig. 2a), Jurassic–Cretaceous carbonate–siliceous (Tb in Fig. 2a) and Cretaceous – early Miocene clayey (Tc in Fig. 2a) and arenaceous (Td in Fig. 2a) succession; (e) the Tuscan Metamorphic Unit consisting of a metamorphic succession composed of the Palaeozoic phyllite–quartzitic Group, the Triassic Verrucano metasiliciclastics Group and Jurassic–Eocene metasedimentary cover (marble, calcschist and phyllite; TM in Fig. 2a).

Boreholes and indirect subsurface data analyses in the basin highlight buried structural highs, both longitudinal and transversal to the basin (Mariani & Prato, 1988; Pascucci *et al.* 2007; Benvenuti *et al.* 2014), separating the depocentre, infilled with more than 1 km of sediments and located in a narrow sector comprised between the western basin shoulder and the valley of the Elsa river (Pascucci *et al.* 2007).

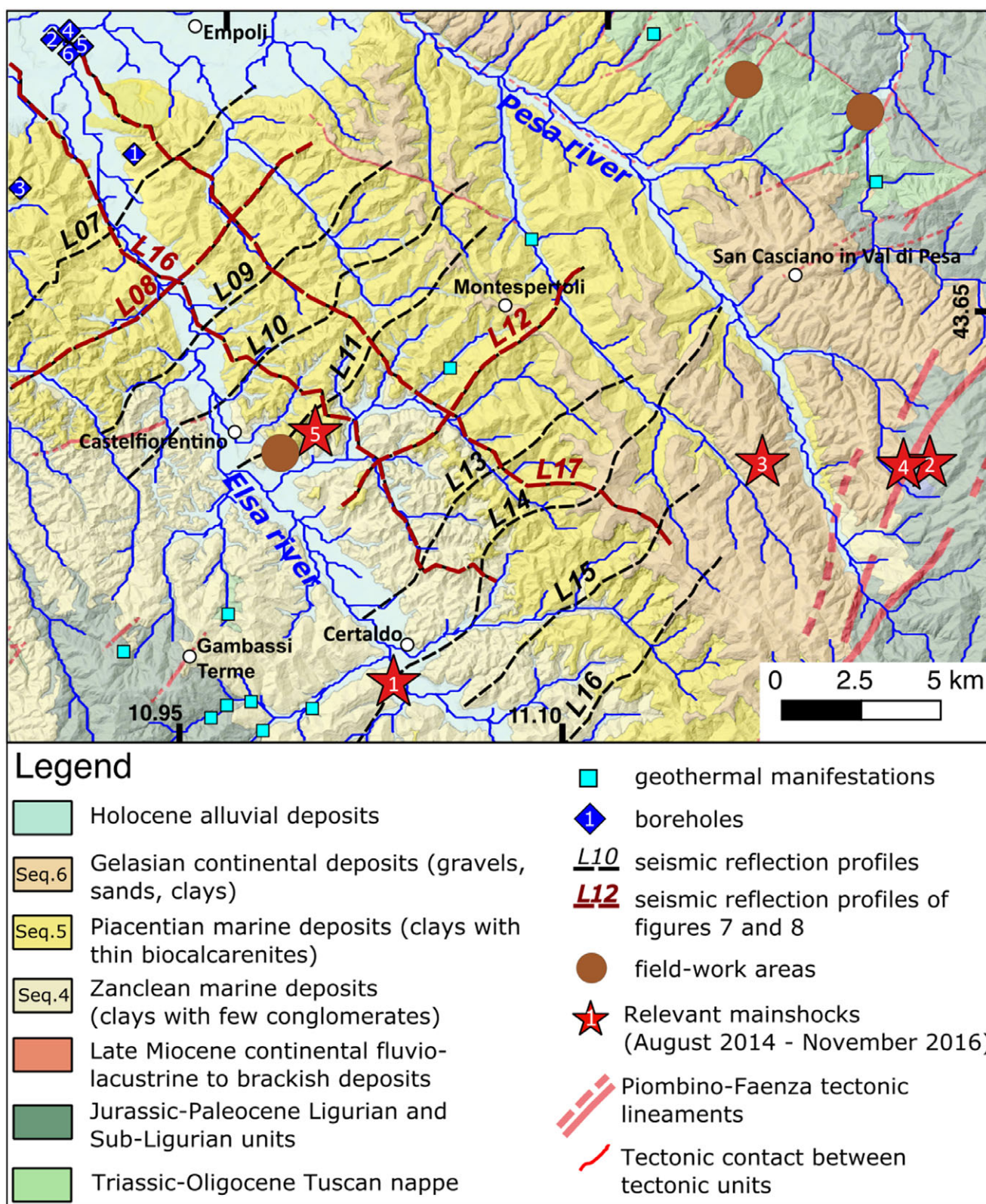


Fig. 3. (Colour online) Geological map of the study area (location in Fig. 1b) showing the distribution of the Neogene deposits, the position of the 2014–16 mainshocks, and the position of the subsurface data used for the subsurface reconstruction (boreholes and seismic reflection profiles). Key to borehole numbers: 1 = Monterappoli; 2 = Certaldo2; 3 = Certaldo3; 4 = Certaldo4; 5 = Certaldo1; 6 = CertaldoSud1.

The whole study area is affected by both NW- and NE-striking faults of regional relevance (Fig. 1b). A mostly continuous SW-dipping normal fault system occurs in the eastern border of

the basin. The fault segments separating the Neogene deposits from the pre-Neogene units are mostly buried, but parallel segments can be recognized within the substratum units (Fig. 1b). Nevertheless,

Table 1. Mainshocks within the study area

Date	Time	Lat. (°N)	Long. (°E)	Depth (km)	Magnitude		Location
9 Aug 2014	13:47:49	43.5367	11.0358	9.9	Mw	3.4	1. Certaldo
19 Dec 2014	10:36:31	43.6058	11.2405	8.6	Mw	4.1	2. Greve in Chianti
4 Mar 2015	00:00:04	43.6038	11.1753	9.2	Mw	3.7	3. Tavarnelle Val di Pesa
13 Sep 2015	01:04:35	43.6047	11.2303	8.9	ML	3.8	4. Tavarnelle Val di Pesa
25 Oct 2016	16:53:01	43.6063	11.0007	10.2	Mw	3.9	5. Castelfiorentino

ML, local magnitude; Mw, moment magnitude. Relevant mainshocks occurring in the period August 2014 to November 2016 in the study area (after <http://terremoti.ingv.it>). The 'Certaldo' (1) and 'Castelfiorentino' (5) events are discussed in more detail in the text and their focal solution is shown in Figure 9.

the prolongation of this fault system, as well as of the basin itself toward the SE, is interrupted in correspondence to the NE-striking Piombino–Faenza tectonic lineament.

The Valdelsa Basin is characterized by heat flow values locally reaching 100 mW m^{-2} (Mongelli and Zito, 1991), in the range of the average value of the southern Tuscany geothermal anomaly (Della Vedova *et al.* 2001). The whole Valdelsa Basin is therefore characterized by geothermal manifestations, consisting of tectonically controlled thermal springs and gas vents (Bencini *et al.* 1979; Fazzuoli *et al.* 1983; Minissale, 2004) mainly concentrated in the Gambassi Terme – Certaldo area and the Montespertoli–Firenze area (Fig. 3) and located along a dominant SW–NE trend. The physico-chemical characteristics of the thermal waters allow some different compositional groups to be recognized. According to several authors (Bencini *et al.* 1979; Celati *et al.* 1990; Fazzuoli *et al.* 1983; Minissale, 2004), the most homogeneous group consists of alkaline-chloride type waters that seem to be mainly controlled by evaporitic processes possibly related to Triassic Burano Fm. Other types of waters, such as the alkaline-bicarbonate type, may reflect interaction with different rocks, from carbonate successions (Ligurian and/or Tuscan units) to Neogene clays.

3.a. Stratigraphy of the Neogene deposits

The sediments cropping out in the Valdelsa Basin consist of Plio-Pleistocene marine and continental deposits. The marine Pliocene sediments, mostly consisting of clay, marl, sand, gravel and conglomerate, are unconformably overlaid by fluvio-lacustrine Pleistocene gravel, sand, clay and locally by Middle–Late Pleistocene continental carbonate (Capezzuoli *et al.* 2005; Capezzuoli *et al.* 2009). The stratigraphic setting of the Valdelsa Basin was classically described through informal lithostratigraphy of an overall regressive trend (Lotti, 1900; Lotti *et al.* 1908; Canuti *et al.* 1966; Merla & Bortolotti, 1967; Merla *et al.* 1967) and biostratigraphically constrained by markers such as planktonic foraminifera, nannofossils (Bossio *et al.* 1993b; Capezzuoli *et al.* 2005) and continental micromammals (Benvenuti *et al.* 1995; Abbazzi *et al.* 2008).

A detailed revision of the tectono-stratigraphic setting was performed by Benvenuti & Degl'Innocenti (2001) and Benvenuti *et al.* (2014), who divided the upper Messinian – Pliocene infilling succession into seven unconformities-bounded stratigraphic units (S1–S7).

We refer to the subdivision of units proposed by Pascucci *et al.* (2007) schematized in Figure 2b as more directly connected to the seismic units described later in the text. According to Pascucci *et al.* (2007), the basin results infilled with up to 1000 m of Late Miocene

and 1000 m of Pliocene deposits (Seq.2 to Seq.5). A deeper Late Serravallian succession (Seq.1) formed by continental to shallow marine sandstone and conglomerate (Ponsano Sandstone Fm; Foresi *et al.* 2003 and references therein), unconformably resting on the basin substratum represented by Ligurian units, was described in discontinuous exposures in the SE portion of the basin (Lazzarotto & Sandrelli, 1977; Pasini & Sandrelli, 1977).

The Late Miocene continental succession unconformably overlies Seq.1 and encompasses Late Tortonian – Messinian fluvial-lacustrine sediments (Seq.2), mainly consisting of clayey-sandy levels and conglomerate with interbedded lignite-level beds ('Serie Lignitifera'), and late Messinian lacustrine clays (Seq.3; S1 of Benvenuti *et al.* 2014) with layers of sandstone and conglomerates occurring mainly in the SE area (Casino Basin; Lazzarotto & Sandrelli, 1977).

Seq.3 is overlain by the Zanclean Seq.4 (S2, S3 of Benvenuti *et al.* 2014) mostly composed of marine clays with a few interstratified conglomeratic layers. Clay dominates the centre of the basin, with the coarser clastic deposits occurring on the margins. The Piacenzian Seq.5 (S4, S5, S6 of Benvenuti *et al.* 2014) is composed of marine clays; thin sandstone units occur at its base and top, where there are also local, thin biocalcarenes.

The above units are overlain by an Early Pleistocene (Gelasian) deposition (S7 of Benvenuti *et al.* 2014) of fluvial drainages deriving from the Chianti Hills.

3.b. Historical and instrumental seismicity

Widespread low-magnitude seismicity characterizes the whole inner zone of the Northern Apennines. The seismic events are mainly confined to the upper crust, at depths ranging from 3 to 10 km (Selvaggi & Amato, 1992; Cameli *et al.* 1993; Di Bucci & Mazzoli, 2002). The Istituto Nazionale di Geofisica e Vulcanologia (INGV) earthquake catalogues CPTI-15 (Rovida *et al.* 2016) and DBMI15 (Locati *et al.* 2021) indicate that the historical seismicity in the area was characterized by several moderate earthquakes, with magnitudes in the Valdelsa Basin up to $M_e = 5.1$ (Fig. 1b).

The strongest seismic event ever reported in the area between Chianti and Valdelsa occurred on 18 May 1895 and had a magnitude of $M_e 5.5$. The intensity reached VIII (MCS) and caused four casualties. In the aftermath, the small locality Sant'Andrea changed its name to Sant'Andrea in Percussina (name derived from 'percussion' to testify to ground shaking). However, recent seismic events with epicentres inside the study area (Castelfiorentino–Certaldo) have not exceeded $M = 4.7$. Recently, four relevant seismic sequences ($3.4 < M < 4.1$) occurred in the area between Valdelsa and Chianti (Table 1).

4. Methods

We integrate available surface structural and kinematic data in the substrate, the interpretation of a set of seismic reflection profiles calibrated with boreholes and the relocation of seismicity to identify possible surface and subsurface evidence of the faults responsible for the most recent seismic sequences. We performed fieldwork along bedrock-hosted fault segments in order to gain information on the fault geometry and kinematics. Fieldwork data were gathered at three main structural sites located in Figure 3.

Based on a detailed revision of the Neogene deposits stratigraphy, we interpreted a set of seismic reflection profiles which cross the Valdelsa basin and which were calibrated with both surface geology and the Monterappoli1 borehole, the closest and most relevant in the area (Fig. 3). The seismic profiles interpretation allowed us to draw a subsurface image of the relevant tectonic structures and to identify and map the Neogene basin depocentre throughout the area.

We relocated the 2014 Certaldo and 2016 Castelfiorentino main shocks of the seismic sequences and plotted the events onto two cross-sections obtained from the depth-converted seismic reflection profiles.

We compared the above-mentioned datasets and interpreted the results into a comprehensive picture of the elusive active faults of the area.

5. Data

5.a. Structural and kinematic data

As the epicentral distribution of the earthquakes is mostly concentrated along a SW–NE-trending tectonic lineament, detailed structural analyses were carried out on a wide area comprehending the central-eastern part of the Valdelsa Basin and its eastern shoulder. Here, structural and kinematic data were collected in a few (due to the scarcity of significant outcrops), though noteworthy, exposures (see locations in Fig. 3). The clay and silt filling the basin, in fact, are not suitable for the development and preservation of fault scarps, as well as the related kinematic indicators. Despite this limitation, mesoscopic faults were analysed in a few exposures made up of unconsolidated clayey deposits, belonging to the Piacenzian marine succession, and on the pre-Neogene units (i.e. Tuscan Nappe and Ligurian units) of the basin substratum, in order to obtain more exhaustive geometric and kinematic information. The collection of these data took place mostly in the substratum, with a few also being collected in the basin infill, and was aimed at avoiding kinematic data derived from pre-Neogene deformational events. Using this approach, independently of the deformed lithotype, rock age and kinematic indicators, the orientation of the analysed mesoscopic faults follows the main trend of the regional-scale structures (Fig. 1b), thus displaying both NW- and NE-striking fault systems.

Kinematics was analysed overall for the NE-trending structures, which are the most recurring structures in the study area. Exposures suitable for kinematic analyses are rare, due to the lithological composition of the Ligurian units mainly formed by shale with interbedded limestone beds. Nevertheless, continuous exposures of sandstone and marl levels were found on fresh cuts along the main roads or within river incisions. More than 50 kinematic data points were collected from three structural stations in three fieldwork areas (see locations in Fig. 3).

In the sandstone and marly rocks of the Tuscan Nappe and Ligurian units, respectively, the bulk of the mesoscale faults are

characterized by a core zone up to 40 cm in size, derived from the comminution of the damaged lithotypes (Fig. 4). The fault damage zone is characterized by well-organized fracture networks defining metre-sized domains, with different amounts of deformation that decrease with distance from the core zone. Kinematic indicators are given by slicken-lines, calcite fibre steps and chatter marks (Fig. 4), arrays of extensional jogs and T-fractures. Kinematic indicators on the NE-striking fault system show at least three superposed movements, at a few structural stations (Fig. 5). Movements range from strike-slip to oblique-slip even if dominant oblique to normal components were recognized. In the basin fill, fault slip surfaces are less widespread due to the dominant clayey and sandy composition of the Neogene sediments. Fault surfaces with clear kinematic indicators were not recognized, but clear NE-striking fault segments were analysed in an abandoned quarry near Castelfiorentino (Fig. 6). Here, the bulk of the meso-faults affecting the unconsolidated sediments are characterized by apparent offsets of a few decimetres and by a thin core (c. 1 cm). Data on fault geometry and kinematics are reported in Figure 5.

Kinematic data from the measured fault surfaces can be used for palaeo-stress analysis, graphically represented by double-couple fault-plane solution diagrams (Angelier, 1979).

In Figure 5, NE-striking oblique-slip faults with right- and left-lateral movements were analysed separately. Right-lateral faults display a maximum compressional axis trending about E–W. The minimum compressional axis is always almost sub-horizontal and trending about N–S. Left-lateral faults display a maximum compressional axis trending about N–S and a minimum compressional axis almost sub-horizontal and trending about W–E.

5.b. Interpretation of seismic lines and basin architecture

We considered a dataset of c. 150 km of seismic data composed of 12 seismic reflection profiles acquired in the 1980s by the Agip oil company (presently ENI), and six boreholes (see locations in Fig. 3). Some of these seismic profiles have been interpreted in the past and some are already published (Pascucci *et al.* 2007; Benvenuti *et al.* 2014). The seismic lines are both longitudinal (NW–SE) and transversal (SW–NE) with respect to the trend of the basin and main geological structures and reach c. 4 s two-way travel time (TWT), corresponding to c. 6 km on the basis of the average subsurface velocities.

The quality of the seismic lines is very good in the upper 2 s TWT due to good penetration of the seismic signal and to the lithological characteristics of the basins infill being mostly made up of both marine and continental sandy and clayey successions.

We interpreted the complete dataset and present the four most representative seismic profiles, which image the subsurface geological setting of the area (Figs 7 and 8). The interpretation of the seismic data was calibrated with the Monterappoli1 well, which is the closest to the study area (location in Fig. 3). The most representative wells in the area (Certaldo1, Certaldo2, Certaldo3, CertaldoSud1 and Certaldo4) were also considered, in order to have a better control on the later continuity of the drilled successions. The Monterappoli1 borehole (publicly available in the VIDEPI PROJECT database – <https://www.videpi.com/videpi/pozzi/consultabili.asp>) was projected onto the closest seismic profile (L17 in Fig. 3), and the main lithological boundaries were associated with the corresponding reflectors. The association between the contacts encountered in the borehole and the seismic profile was made by using the stacking interval velocities, which

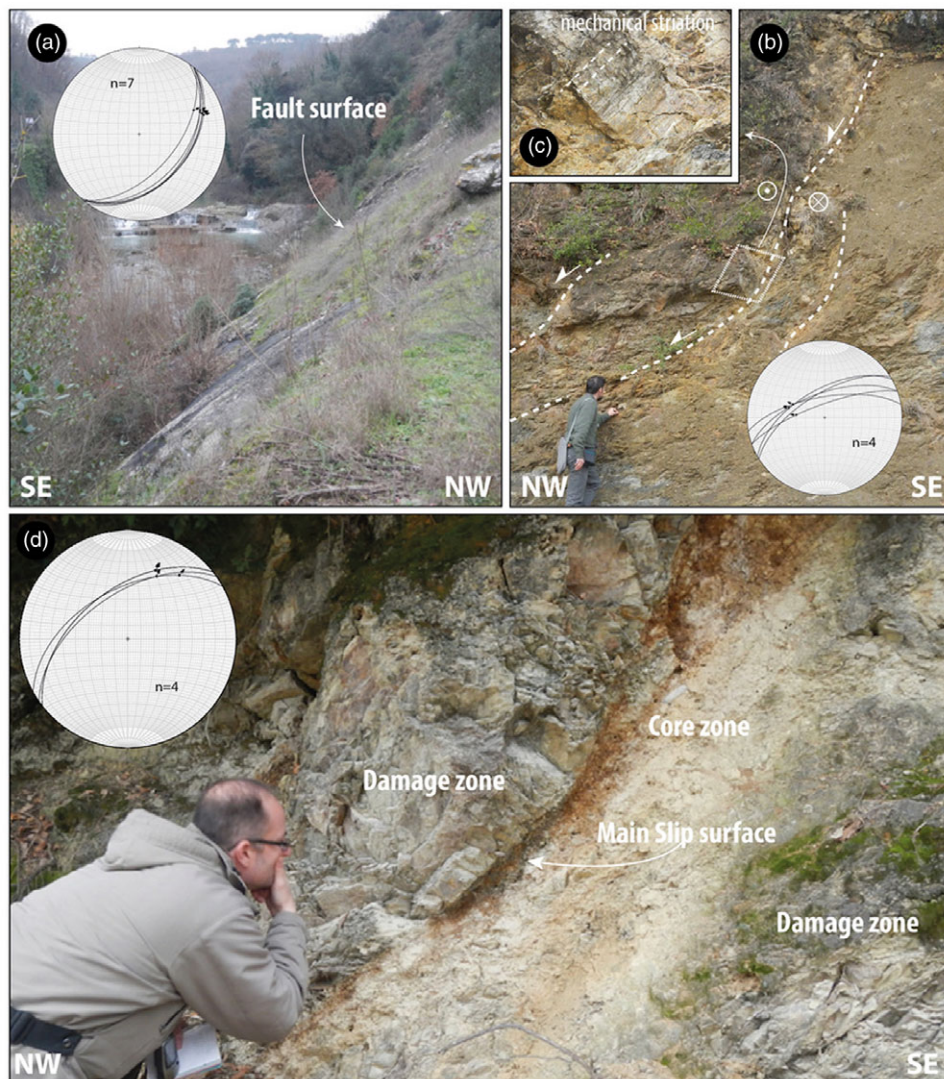


Fig. 4. (Colour online) Examples of mesoscopic-scale fault analysed north of San Casciano Val di Pesa (see Fig. 3 for location): (a) SE-dipping transensional left-lateral fault affecting late Oligocene sandstone of the Tuscan Succession; (b) outcrop-scale transensional left-lateral NW-dipping fault affecting alternated limestone beds and shale of the Ligurian units; (c) detail of the kinematic indicators in (b) showing transensional left-lateral kinematics; (d) NW-dipping right-lateral oblique-slip fault zone showing a core c. 50 cm thick surrounded by metres-thick damage zone affecting marly limestone of the Ligurian units. Stereographic diagrams (lower hemisphere, equal area) indicate fault and striae measured in the fault surfaces shown in the photographs.

were compared with the available data for these units (Bally *et al.* 1986; Buonasorte *et al.* 1988; Barchi *et al.* 1998). On this basis we consider two main velocity bodies, the Pliocene ($V_p \sim 2.6 \text{ km s}^{-1}$) and the Miocene ($V_p \sim 3.5 \text{ km s}^{-1}$). Thus, we use these interval velocities to estimate the depth and thickness of the sedimentary infill of the basin.

We identify three main seismic units of the Valdelsa Basin (Fig. 2b), which are easy to identify in the seismic profiles and which we relate to the stratigraphic sequences described above and represented in Figure 2b. From top to bottom, these are: (i) Seismic Unit A (SU-A, Fig. 2b), corresponding to the late Serravallian, continental-to-shallow marine Seq.1 sequence (Ponsano Fm); (ii) Seismic Unit B (SU-B, Fig. 2b), including the Seq.2 and Seq.3 Tortonian–Messinian continental succession; and (iii) Seismic Unit C (SU-C, Fig. 2b), including Seq.4, 5, 6 and corresponding to the Pliocene marine deposits and the Gelasian continental deposits.

Based on the extrapolation of the boundaries between the seismic units along the seismic profiles and the corresponding seismic profile intersections, we were able to derive a consistent interpretation of the subsurface geological setting of the area, synthesized in two transversal SW–NE-trending seismic reflection profiles (line 8 and line 12; Fig. 7a and b) and two longitudinal NW–SE-trending profiles (line 16 and line 17; Fig. 8a and b).

The oldest seismic unit is Seismic Unit A (SU-A), which in the seismic profiles is represented by light seismic facies with a series of easily recognizable and continuous reflectors and a few higher-amplitude horizons (Fig. 8c).

The intermediate seismic unit (Seismic Unit B, SU-B) is represented by a less light and transparent seismic facies and an upper part characterized by a set of well-bedded and higher-amplitude reflectors (Fig. 8c) possibly representative of the more clayey upper Miocene lacustrine unit (Seq.3 in Fig. 2b). The uppermost seismic unit (Seismic Unit C, SU-C) is represented by an alternation of

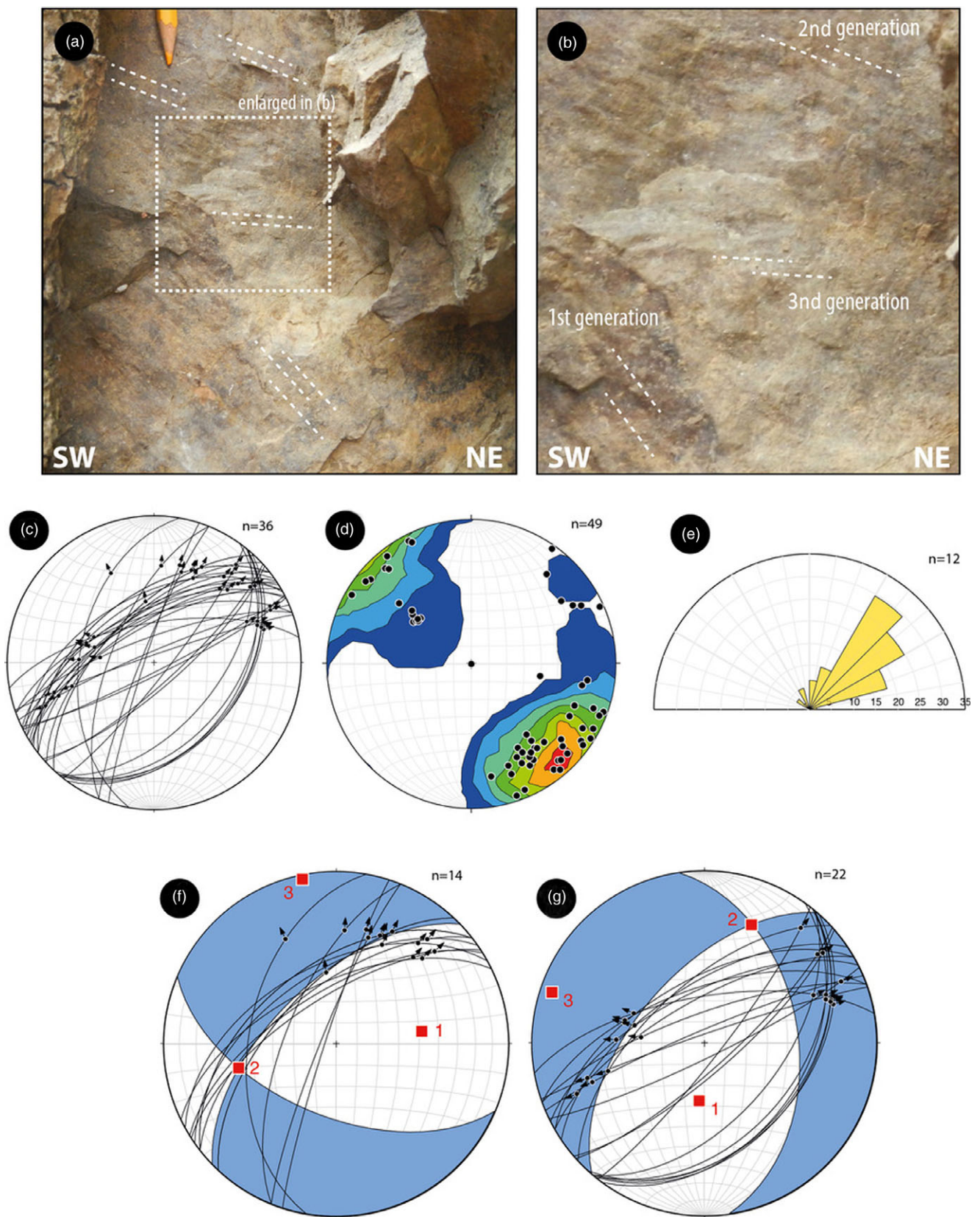


Fig. 5. (Colour online) (a) Superposed kinematics indicators on a fault surface in late Oligocene sandstone north of San Casciano Val di Pesa (see Fig. 3 for location); (b) detail of three generations of movements; (c) stereographic diagrams (lower hemisphere, equal area) indicating the representative fault and striae measured in the measured fault; (d) density contours of fault poles; (e) fault strikes rose diagrams; (f, g) palaeo-strain analysis using the right-diedra method (Angelier, 1979) obtained with Faultkin application (Marrett and Allmendinger, 1990; Allmendinger *et al.* 2012) showing fault-plane solutions and main kinematic axes.

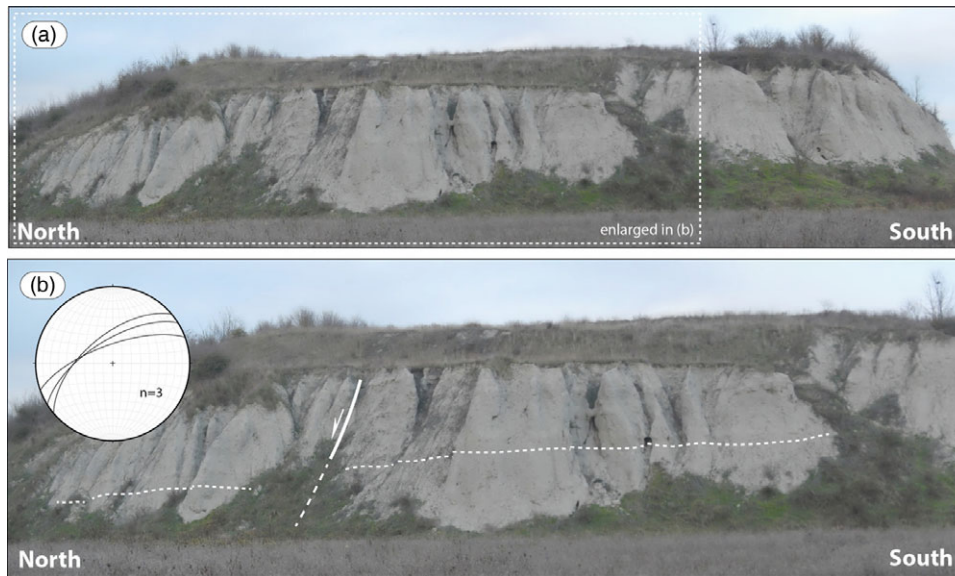


Fig. 6. (Colour online) NE-striking fault segments in an abandoned quarry near Castelfiorentino (see Fig. 3 for location). The apparent offsets in the unconsolidated sediments are of a few decimetres and from a c. 1 cm thin core.

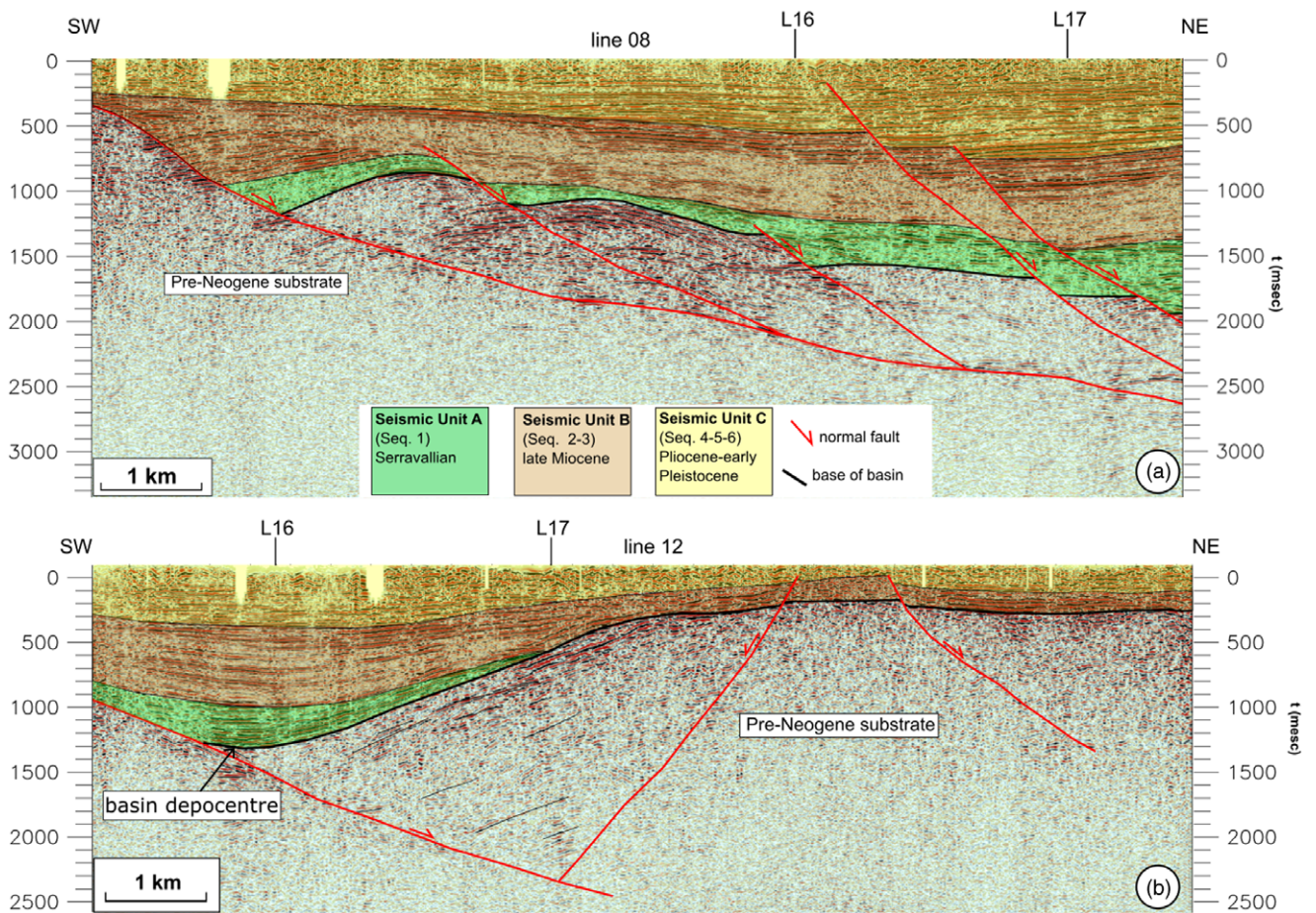


Fig. 7. (Colour online) Geological interpretation of seismic lines L8 (a) and L12 (b) (see Fig. 3 for location) showing the deep geometry of the Valdelsa Neogene deposits and their relationships with the main extensional structures of the area.

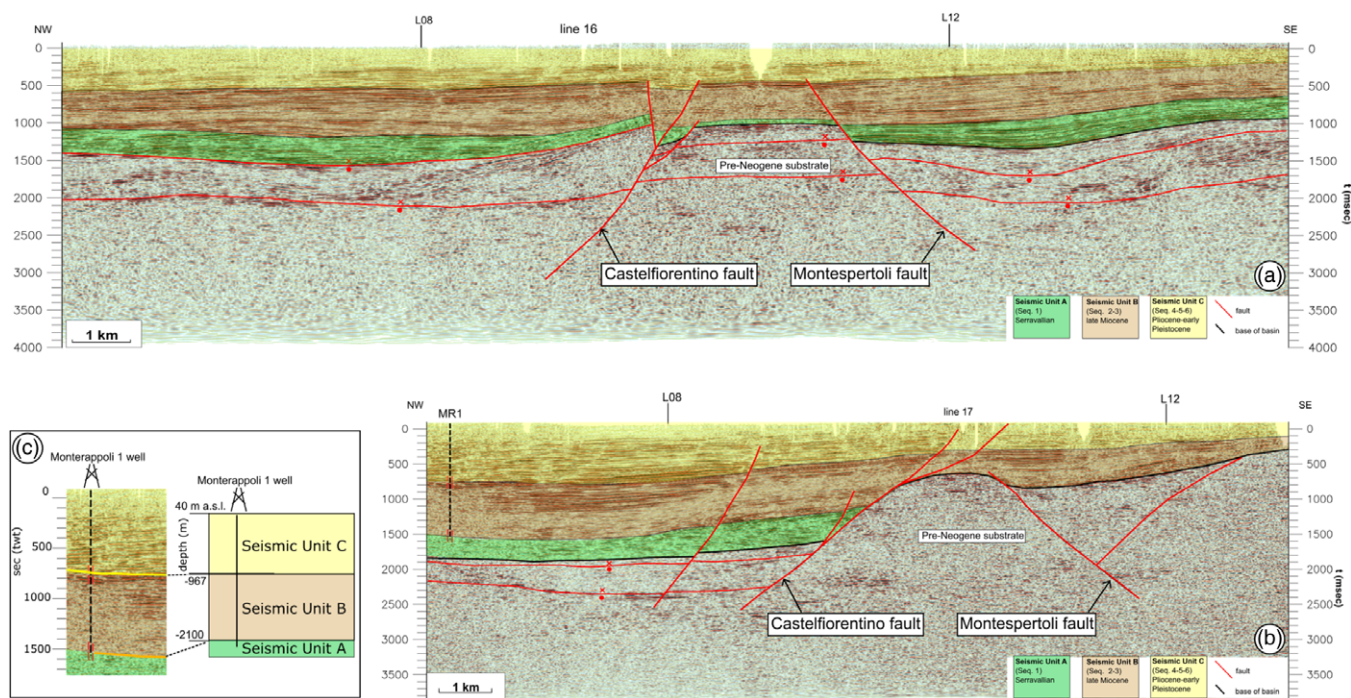


Fig. 8. (Colour online) Geological interpretation of seismic lines L16 (a) and L17 (b) (see Fig. 3 for location) showing the longitudinal deep geometry of the Valdelsa Neogene deposits and their relationships with two main faults (Castelfiorentino and Montespertoli), which controlled the most recent thickness of the Valdelsa infill. The position of the intersections with seismic lines L8 and L12 (Fig. 6) is also reported. The Castelfiorentino and Montespertoli faults interrupt the depth trace of the main normal faults of seismic lines L8 and L12 post-dating them. (c) Seismic stratigraphy of the Monterappoli-1 well and association with the seismic units (SU).

continuous high-amplitude layers and layers that are still continuous but are lighter than the underlying deposits (Fig. 8c).

The transversal profiles provide an image of the architecture of the extensional basins showing the presence of an ENE-dipping extensional detachment with associated synthetic splays and subordinate antithetic faults. The oldest unit at the normal faults hangingwall is represented by the Serravallian Seq.1, which unconformably overlies the pre-Neogene substrate (Fig. 7a). This sequence is not always present in the subsurface, as shown by line 12 (Fig. 7b) where in the central part of the section the substrate is overlaid directly by SU-B (probably only the upper Miocene lacustrine Seq.3).

The Neogene sediments reach a thickness in the order of 2 km, progressively diminishing to a few hundred metres.

The longitudinal seismic sections (Fig. 8) provide an excellent image of the lateral continuity of the Neogene deposits from NW to SE. Seismic line 16 (Fig. 8a), running SW of line 17 (Fig. 8b) and hence closer to the present-day Elsa river valley, is the longest and shows the thinning of the sequences, especially of SU-A corresponding to a pre-Neogene structural high bounded by two sub-vertical faults. The substrate structural high in the central part of the section is responsible for the thinning of the sequences, especially of SU-A, and is bounded by a NW-dipping and a SE-dipping fault, here named Castelfiorentino and Montespertoli faults, respectively. The Neogene deposits are much thicker SE of the substrate high and reach a maximum thickness in the order of 2 km.

Seismic line 17 (Fig. 8b) shows that the same pre-Neogene structural high here is higher and causes all the seismic units, especially SU-A, to thin abruptly towards the SE. The maximum thickness of all the Neogene sediments is *c.* 1.8 s TWT, corresponding to *c.* 2 km on the basis of the available information on the seismic

velocities. The thickness reduces to a few hundred metres in the southeastern part of the sections.

5.c. Seismological data

We relocated the two most recent moderate earthquakes, which struck the area in 2014 and 2016, the Certaldo and Castelfiorentino earthquakes, respectively.

5.c.1. The Certaldo seismic sequence ($M = 3.4$; 9 August 2014)

After a short foreshock sequence of 8 hours, a seismic event of $M = 3.4$ occurred in the central part of the Valdelsa Basin (near Certaldo; Fig. 3; Table 1) on 9 August 2014 at 13:47 UTC. The main shock was located at a depth of 9 km and was followed by a short-lived aftershock sequence of *c.* 40 events, which ceased after less than a week. Due to the shallow hypocentral depths of 5–10 km, about a dozen earthquakes were felt by the population. The seismic source mechanism was calculated by first-motion polarities, as well as Moment Tensor Inversion (MTI), and resulted as a pure double couple with the following parameters: strike 74° , slip 88° , rake 170° (Fig. 9).

5.c.2. The Castelfiorentino earthquake ($M = 3.9$; 25 October 2016)

Two years later, a further seismic sequence of *c.* 160 events shattered the NW shoulder of the Valdelsa Basin (Fig. 3). After isolated and sporadic events since January, during October 2016 the seismic activity increased significantly, culminating in the $M = 3.9$ main shock on 25 October 2016 at 16:53 UTC. The epicentre of the main shock was localized at Castelfiorentino, 10 km NNW with respect to the Certaldo sequence, at a hypocentral depth of 9 km. The calculation of the source mechanism, both

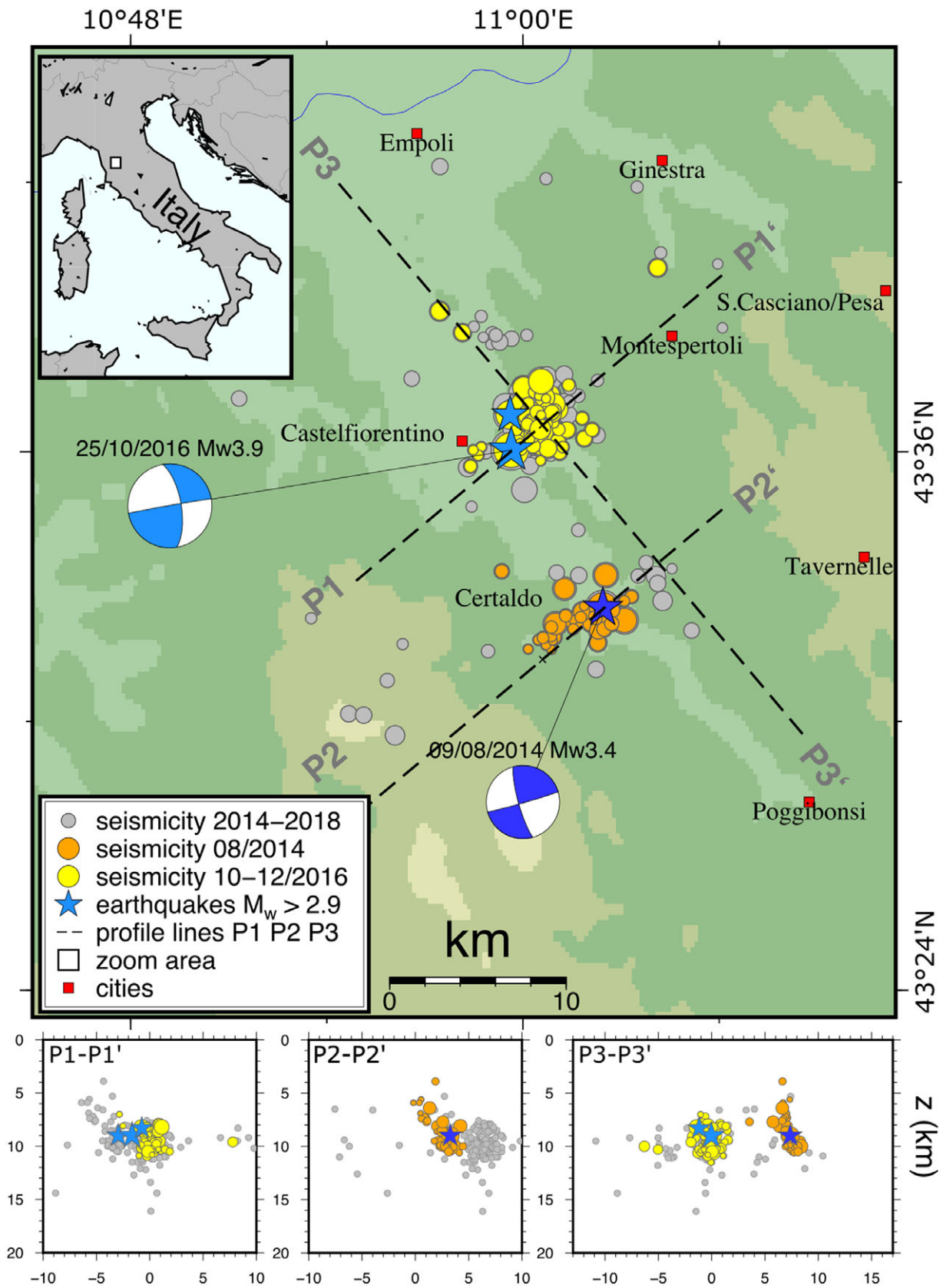


Fig. 9. (Colour online) Distribution of the 2014 Certaldo and 2016 Castelfiorentino seismic sequences relocated in this work, and the mainshock focal mechanisms showing either a dextral SW-NE-trending or a sinistral NW-SE-trending kinematics. The seismicity distribution at depth is imaged by the P1, P2 and P3 cross-sections.

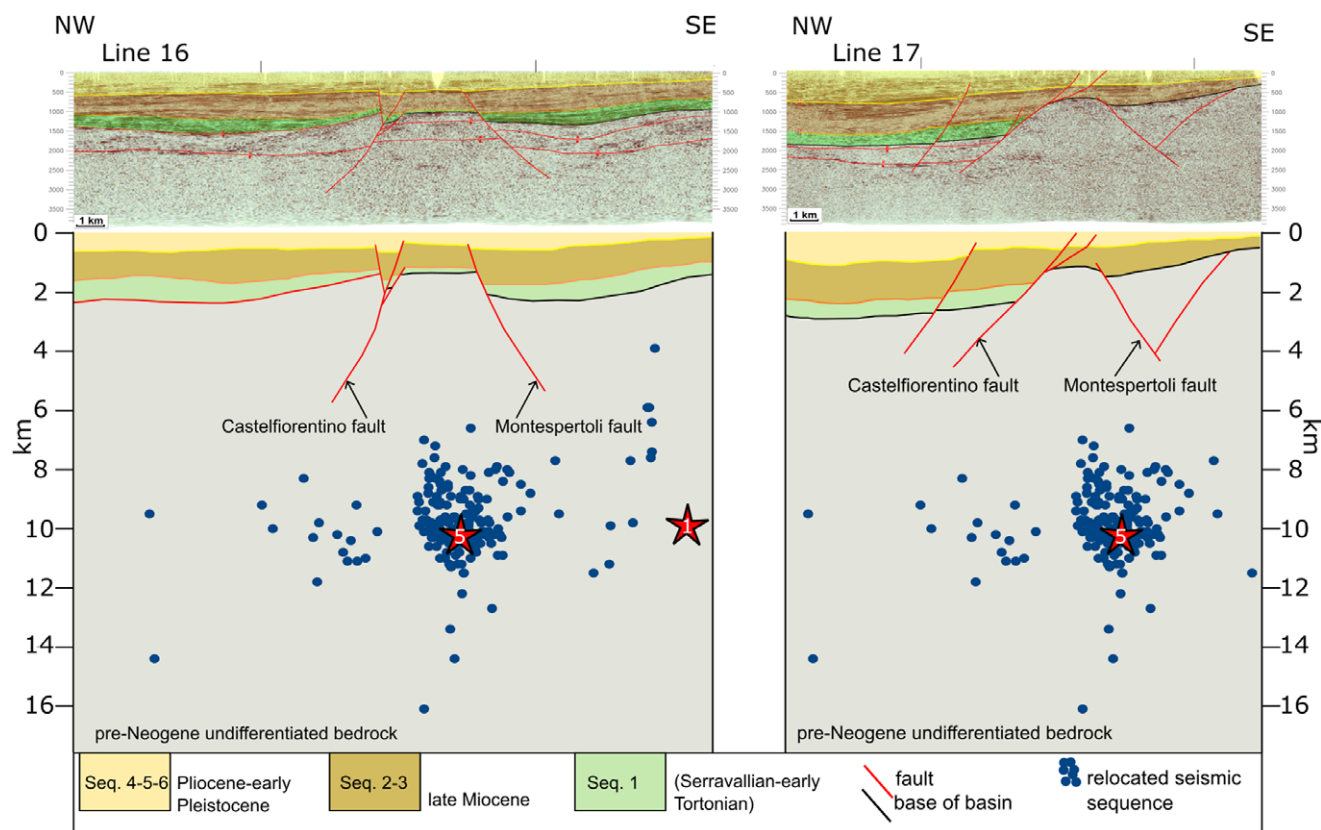


Fig. 10. (Colour online) Depth conversion of seismic lines L16 and L17 and projection of the relocated seismicity and mainshocks onto the depth-converted cross-sections. See text for details and data discussion.

by the inversion of first-motion polarities and by MTI, produced a result similar to that for the Certaldo main shock: strike 260° , dip 89° , slip 158° .

The two seismic sequences show striking similarities: the hypocentres of the main shock are located at *c.* 9 km and the fore- and aftershocks are confined to the upper crust. The source mechanisms of the main shocks are pure double couples, with a predominant strike-slip mechanism: nearly N–S (left lateral, P3) or rather E–W-striking (right lateral P1, P2 in Fig. 3), whose active fault plane cannot be irrefutably determined (Fig. 9).

6. Results

Using the seismic velocities of the deposits, we converted to depth the two longitudinal sections and we drew two integrated geological cross-sections extrapolated down to *c.* 5 km depth in order to compare the subsurface geometries with the earthquake locations (Fig. 10).

The earthquakes are distributed at *c.* 10 km depth and do not show a clear planar geometry, mostly as a consequence of their low intensity and of the fact that they are not associated with a moderate or strong event during which a set of hundreds or thousands of aftershocks develop and are often aligned along planes, which can be associated with the main fault rupture (see e.g. Latorre *et al.* 2016; Valoroso *et al.* 2017; Michele *et al.* 2020). Nevertheless, the relocated earthquakes plotted onto the geological section show that seismicity is located below the Castelfiorentino and Montespertoli faults at similar depth for both sequences

(Certaldo 2014, $M = 3.4$ and Castelfiorentino 2016, $M = 3.9$), even if slightly shifted below the Montespertoli fault (Fig. 10).

The resolution of the seismic reflection profiles does not allow offsets younger than the early Pliocene to be seen, so in order to verify the possible role of the SW–NE-striking Castelfiorentino and Montespertoli faults in controlling the Neogene basin dimension or in displacing its position, we mapped both the Neogene depocentre throughout the whole seismic lines dataset and the surface projection of the SW–NE-striking Castelfiorentino and Montespertoli faults footwall cut-offs (see Fig. 8a and b) with the substrate (the base of basin deposits).

The results are illustrated in Figure 11. The map shows the seismic lines dataset and the position of the surface projection of these two key elements. It can be observed that the faults cut-offs projection at surface depicts the Castelfiorentino and Montespertoli faults strike, which is SW–NE, about $N40^\circ$.

The Castelfiorentino and Montespertoli faults border a structural high (Castelfiorentino High of Benvenuti *et al.* 2014) constituted by the pre-Neogene substrate with a steep to sub-vertical geometry in cross-section (Fig. 10). At surface, the Certaldo and Montespertoli faults show a trend of *c.* $N40^\circ$, similar to the strikes of the focal mechanisms of both the Certaldo and Castelfiorentino earthquakes (Fig. 9).

The position of the Neogene depocentre provides interesting points of discussion. The first thing to observe is that the present-day Elsa river is systematically shifted to the west with respect to the Neogene depocentre (Fig. 11). A similar situation was previously observed for the northeastern Quaternary basins of the Tiber river (Pucci *et al.* 2014) and interpreted as due to

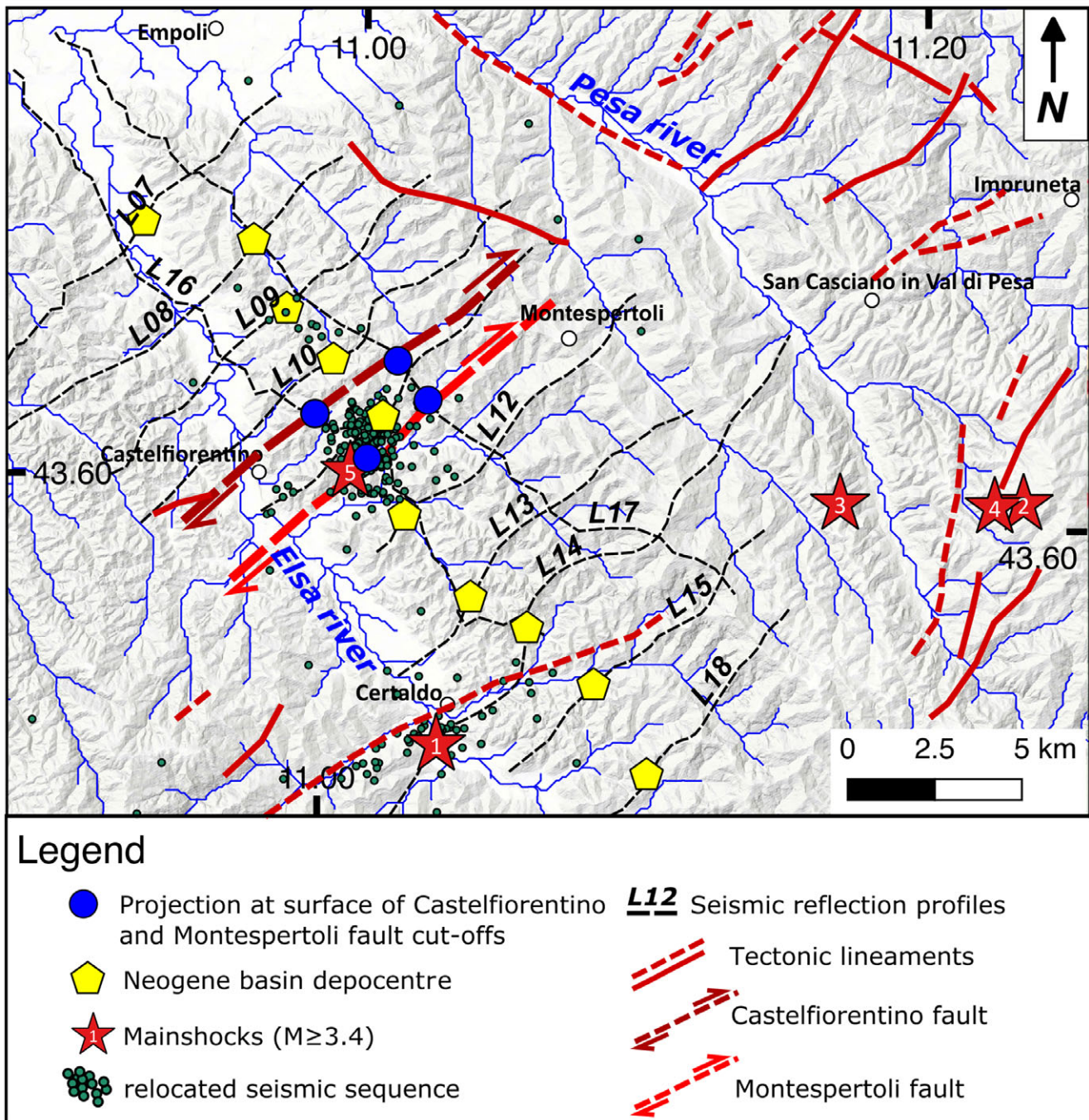


Fig. 11. (Colour online) Surface projection of the pre-Neogene substrate fault footwall cut-offs (blue circles), of the Neogene basin depocentre and the relocated seismicity. The figure shows the relationship between the distribution of seismicity, the Castelfiorentino earthquake position and dextral shift of the Neogene basin depocentre suggesting that the Montespertoli fault (thick red dotted dextral fault) was responsible for the 2016 seismic sequence. Both the Castelfiorentino and the Montespertoli fault trends agree with the other SW-NE trending of the region.

the continuous activity of the basin-bounding normal faults, and in particular to the NE-dipping normal faults. The second observation is that the alignment of points corresponding to the position on the Neogene depocentre in the seismic profiles is not continuous along a NW-SE direction but is divided into two parts and shifted right-laterally, corresponding to the valley connecting the Elsa river and the village of Montespertoli, between seismic lines L11 and L12 (Fig. 11). This shift also corresponds to the footwall cut-offs alignment of the Montespertoli fault.

These observations indicate that: (i) the Valdelsa Basin Neogene deposition is controlled by the NW-SE-trending normal faults clearly visible in the seismic reflection profiles (Fig. 7); (ii) extension was accommodated mostly by the NE-dipping faults, which were able to progressively drag the depocentre to the NE and at the same time to maintain the Elsa river at its position, at the normal-fault hangingwall; (iii) there occurred a later deformation ascribable to a SW-NE-trending fault, which displaced the Neogene depocentre original trend. Given the above-mentioned

points, we suggest that the SW–NE-striking Montespertoli fault is capable of shifting the depocentre of the basin horizontally by c. 1.2 km with right-lateral kinematics (Fig. 11). Given the fault geometry, which dips to the SE, the resulting movement would be right-lateral or slightly transtensional.

The observation of the drainage pattern distribution of the study area seems to be in agreement with a fault control on the river network. The drainage pattern is mostly oriented SE–NW and associated with the Elsa and Pesa rivers (Fig. 11). A few areas, where the rivers show a significant deviation from the dominant SE–NW trend, differ in terms of drainage orientation and display tight curves along a SW–NE direction of flow. The three most evident SW–NE alignments in the study area are along the previously mentioned Piombino–Faenza line to the south, along the Certaldo – S. Casciano Val di Pesa area and along the Castelfiorentino area (Fig. 11).

Given the seismic sequence relocation and the 2016 Castelfiorentino focal mechanism solution, we suggest that the fault, which ruptured in 2016, striking SW–NE with a right-lateral kinematics, corresponds to the Montespertoli fault. Similarly, we propose that the 2014 $M_w = 3.4$ earthquake could have activated another SW–NE-trending fault belonging to the same fault segments pertaining to the Piombino–Faenza lineament. The same fault and/or fault segments may be responsible for the other earthquakes in the area, especially for the 2015 Tavarnelle Val di Pesa, $M_w = 3.7$ event.

At surface, these faults are parallel to the fault segments analysed in the eastern shoulder of the basin, in the vicinity of Impruneta – San Casciano Val di Pesa (Fig. 11). Similarly, the identified faults are parallel to the ‘Piombino–Faenza’ shear zone, implying a reasonable genetic relationship between them.

7. Discussion

The widespread seismicity recorded in the SE sector of the Valdelsa Basin, with hypocentral distribution in the focal depth range from 8 to 12 km (Fig. 10), supports the existence of active NE-striking fault segments in the central-southern sector of the basin. Faults related to the seismic events were identified in the presented seismic profiles (Figs 7 and 8) and delimit a NE-trending structural high buried underneath the Pliocene sediments. These faults did not directly rupture the topographic surface, indicating that the fault segments are characterized by small offsets, as also supported by the low-magnitude seismicity. The analysed fault segments in the basin shoulder, in fact, highlight metres or decametres offsets and show mineralization on the fault planes (e.g. calcite slicken-fibres, Figs 4–6). This evidence supports a fault activity occurring at deeper structural levels, implying that the studied fault zones were progressively uplifted and exhumed after their development, hence testifying to their long-lasting activity. Nevertheless, these structures although indicating a variable kinematics through time, show dominant NE-striking strike- to oblique-slip movements, comparable to the focal mechanisms of the seismic events (Fig. 9). This supports the fact that the Certaldo and Castelfiorentino faults, along which the 2014–16 hypocentres are localized, are part of a long-lived fault system inherent to the ‘Piombino–Faenza’ shear zone. In this view, a Neogene–Quaternary activity under the same regional stress field can be envisaged to promote exhumation of the basin shoulders and the segmentation of the basin. In fact, both the NE- and NW-striking faults controlled the development of the Valdelsa Basin (Pascucci *et al.* 1999) as well as the whole Neogene structural

depressions of the inner Northern Apennines (Martini & Sagri, 1993). NW-striking faults controlled the development of the structural depression while the NE-striking ones accommodated the different amount of extension (i.e. transfer zones).

The age and role of transversal lineaments in the Northern Apennines have long been discussed (e.g. Fazzini & Gelmini, 1982; Bemporad *et al.* 1986; Liotta, 1991; Pascucci *et al.* 2007) and their impact in controlling low-magnitude earthquakes has also been highlighted for northern Tuscany (e.g. Molli *et al.* 2021). Many of these ‘lineaments’ are ascribed to the presence of lithotypes, which react differently to erosion, as could be the case of the ‘Piombino–Faenza line’. Nevertheless, the Certaldo – S. Casciano Val di Pesa and Castelfiorentino lineaments documented here do not show any direct connection with lithology or bedding attitude and could just be related to the presence of SW–NE-trending tectonic structures, as also supported by the seismicity concentrated along their traces.

On the other hand, both NE- and NW-striking faults seem to have controlled the orientation of the main river/stream valleys in the whole basin (Fig. 3). In our case, the two NE-trending lineaments correspond to relevant NE–SW river alignments, along which geothermal manifestations are present (see Fig. 3), supporting their connection with both a tectonic origin and a crustal relevance also in controlling geothermal fluids circulation. Interestingly, a tectonic control on the river network of the same area was early recognized by Canuti *et al.* (1975), though not framed into an active tectonic significance of the river anomalies.

The collected kinematics coupled with information from the focal mechanisms related to the local seismicity indicate that the two orthogonal faults acted mainly as normal faults (NW-striking) and strike-slip/oblique-slip faults (NE-striking) and this interplay accounts for an extensional evolution of the basin (Martini & Sagri, 1993; Pascucci *et al.* 1999). A different scenario was proposed by Benvenuti *et al.* (2014) that, although similarly depicting the occurrence of ‘basin-transverse lineaments’ separating the Valdelsa Basin into two sub-basins, suggests that the whole basin was strictly controlled by NW-trending regional thrusts that controlled the depocentres location as well as the sedimentation. The interplay between compressional tectonics and eustatic sea-level fluctuations are invoked as dominant factors forcing the deposition of sedimentary cycles at the basin scale. In this scenario, the Valdelsa Basin is not considered an extensional basin but a thrust-top basin developed during compressional tectonics since the Late Miocene. This hypothesis is in line with those advanced by some authors (e.g. Boccaletti & Dainelli, 1982; Bonini & Sani, 2002; Finetti, 2006), who refer to the Neogene–Quaternary tectonic evolution of Tuscany as being strictly controlled by unceasing compressional tectonics active since the late Cretaceous and giving rise to different generations of thrusts and back-thrusts and associated thrust-top basins (e.g. Bonini *et al.* 2001; Finetti *et al.* 2001).

Our data contrast with the hypothesis of Benvenuti *et al.* (2014) and support a different structural and kinematic scenario. The fault kinematics in the exhumed basin shoulder accounts for Neogene–Quaternary normal and strike-/oblique-slip faults. Thrusts occurrence is only suggested by the stacked units forming the orogenic pile, but these tectonic contacts, interpreted as low-angle normal faults by other authors (Carmignani *et al.* 1994; Liotta *et al.* 1998), are dissected by both NE- and NW-trending faults occurring at the basin scale and documented in this paper. So, in our opinion, a Neogene–Quaternary extensional evolution can better explain the setting of the Valdelsa Basin and therefore its seismo-tectonic framework and the overall thinned crust well documented

by geophysical datasets (e.g. Pauselli *et al.* 2006). Along the same line, the reasons why the geological evolution of the Valdelsa Basin and the whole inner Northern Apennines is better framed in an extensional setting rather than a compressional one is reported in some papers (Brogi *et al.* 2005; Brogi & Liotta, 2008; Barchi, 2010; Liotta & Brogi, 2020; Brogi, 2011, 2020) to which the reader is addressed for a more exhaustive discussion.

The NE-striking faults, both exposed and inferred by seismological analyses (Fig. 9), are parallel to the Piombino–Faenza line regional structure (Fig. 1b), a first-order structure crossing the whole of the Northern Apennines (Ambrosetti *et al.* 1978; Boccaletti *et al.* 1985) and interpreted, in the inner zone, as a kilometre-wide, crustal-scale transfer zone accommodating extension since the Late Miocene (Liotta, 1991; Dini *et al.* 2008; Liotta *et al.* 2015). The geometry and kinematics of the fault segments forming this transfer zone were constrained in the Larderello geothermal area, to the southwest of the study area (Fig. 1a), where such a structure plays a fundamental role in controlling fluid flow, heat flux and magma emplacement at depth (Gola *et al.* 2017; Liotta & Brogi, 2020). Similarly to the study area, in the Larderello geothermal area the fault segments were active during the Neogene and are still active (Liotta & Brogi, 2020 for a review), as indicated by the localized low-magnitude seismicity (Batini *et al.* 1985; Albarello *et al.* 2005; Bagagli *et al.* 2020).

The kinematics of this transfer zone is the result of superimposed movements through the Neogene–Quaternary, as a consequence of the role of this structure in separating crustal sectors with different amounts of extension and differentiated uplift (Liotta & Brogi, 2020). It follows that the fault segments forming the transfer zone are characterized by multiple kinematics, ranging from strike-slip to normal, also with intermediate kinematics. Similar evidences have been documented for several transfer zones in the whole of the inner Northern Apennines (e.g. Brogi *et al.* 2013; Liotta *et al.* 2015), producing seismicity (Buonasorte *et al.* 1991; Brogi & Fabbrini, 2009; Brogi *et al.* 2014; Piccardi *et al.* 2017). We observe the same evidence for the NE-striking faults exposed in the study area.

This work, even though it deals with relatively small-magnitude events, evidences the importance of integrating different datasets and approaches to identify active or potentially active faults. Their recognition is fundamental in particular for those areas with a history of earthquakes but without recent events. In these areas, characterized by high vulnerability, with great exposure of human lives, infrastructure and historical heritage, the definition of such potentially active faults plays a fundamental role in the definition of seismic hazard and in the protection and conservation of historical and artistic heritage. Examples in Italy are the important cultural centres of Assisi and Norcia in the Northern Apennines, which are located close to recognized seismogenic faults and have historically suffered repeated damages due to strong earthquakes (see for instance the seismic sequences of Colfiorito in 1997–8, L'Aquila in 2009, Ferrara in 2012 and Norcia in 2016).

In the study area the city of Florence and its surroundings, a world-famous UNESCO site, was characterized by a $M = 5.4$ event (18 May 1895) which, despite its moderate magnitude, caused significant damage (Cioppi, 1995; Guidoboni & Ferrari, 1995) and for which no causative fault has yet been mapped.

Our study suggests that the recognized faults could be related to NE–SW alignments potentially connected to the 1895 event, for which damage maps indicate a possible SW–NE alignment (Cioppi, 1995). However, detailed and modern studies would be needed in order to understand the active tectonics indicators,

which must be hidden in both surface and subsurface geological evidence for the area.

8. Conclusions

We identify a long-lived Miocene–Holocene SW–NE-trending fault system in southern Tuscany, which affects the Neogene Valdelsa Basin developed at the hangingwall of NW–SE-trending normal faults. The SW–NE-trending fault system has played the role of transfer zone since the Miocene and consists of both exhumed and blind, still active, fault segments. Through a multi-disciplinary approach, integrating surface kinematic data, subsurface geophysical and geological data and the relocation of seismological data we identify a previously unknown active fault (Montespertoli faults) not reaching the topographic surface, which we interpret as responsible for the 2016 Castelfiorentino ($M = 3.9$) earthquake (western Northern Apennines of Italy). Despite the relatively small magnitude of the event, the Montespertoli fault is part of the much wider SW–NE-striking crustal shear zones developed across the western part of the Italian peninsula (the Livorno–Sillaro and Piombino–Faenza tectonic lineaments; Fig. 1b) that have also controlled the tectono-sedimentary evolution of the Neogene–Quaternary basins since the Middle–Upper Miocene (Bossio *et al.* 1993a). This crustal shear zone has also controlled the emplacement of felsic magmatic intrusion since the Pliocene (Farina *et al.* 2010) and still controls the seismicity and geothermal circulation in the Larderello area (Liotta & Brogi, 2020), thus testifying to its seismotectonic relevance.

We suggest that the earthquake that struck the historic city of Florence in 1895 ($M = 5.4$) and which caused severe damage to both buildings and works of art may have been linked to the same NE-striking crustal shear zone.

Acknowledgements. We thank ENI for providing the seismic reflection profiles. We thank Giovanni Toscani and an anonymous reviewer for thoughtful and constructive reviews, and the editor Olivier Lacombe for editorial assistance.

References

- Abbazi L, Benvenuti M, Ceci ME, Esu D, Faranda C, Rook L and Tangocci F (2008) The end of the 'Lagomare' event in the SE Valdelsa Basin (Central Italy) between local tectonism and regional sea-level rise. *Geodiversitas* **30**, 611–39.
- Acocella V and Fucicello R (2006) Transverse systems along the extensional Tyrrhenian margin of central Italy and their influence on volcanism. *Tectonics* **25**, TC2003. doi: 10.1029/2005TC001845.
- Albarello D, Batini F, Bianciardi P, Ciulli B, Spinelli E and Viti M (2005) Stress field assessment from ill-defined fault plane solutions: an example from the Larderello Geothermal Field (western Tuscany, Italy). *Bollettino della Società Geologica Italiana* **3**, 187–93.
- Alessandrini B, Filippi L and Borgia A (2001) Upper-crust tomographic structure of the Central Apennines, Italy, from local earthquakes. *Tectonophysics* **339**, 479–94.
- Allmendinger RW, Cardozo N and Fisher D (2012) *Structural Geology Algorithms: Vectors & Tensors*. Cambridge: Cambridge University Press.
- Ambrosetti P, Carboni MG, Conti MA, Costantini A, Esu D, Gandin A, Girotti O, Lazzarotto A, Mazzanti R, Nicosia U, Parisi G and Sandrelli F (1978) Evoluzione paleogeografica dei bacini tosco-umbro-laziali nel Pliocene e nel Pleistocene inferiore. *Memorie della Società Geologica Italiana* **19**, 573–80.
- Angelier J (1979) Determination of the mean principal directions of stresses for a given fault population. *Tectonophysics* **56**, T17–26.
- Armijo R, Meyer B, King GCP, Rigo A and Papanastassiou D (1996) Quaternary evolution of the Corinth Rift and its implications for the Late

- Cenozoic evolution of the Aegean. *Geophysical Journal International* **126**, 11–53. doi: [10.1111/j.1365-246X.1996.tb05264.x](https://doi.org/10.1111/j.1365-246X.1996.tb05264.x).
- Bagagli M, Kissling E, Piccinini D and Saccorotti G** (2020) Local earthquake tomography of the Larderello-Travale geothermal field. *Geothermics* **83**, 101731. doi: [10.1016/j.geothermics.2019.101731](https://doi.org/10.1016/j.geothermics.2019.101731).
- Bally AW, Burbi L, Cooper C and Ghelardoni R** (1986) Balanced sections and seismic reflection profiles across the Central Apennines. *Memorie della Società Geologica Italiana* **35**, 257–310.
- Barchi M, Feyter AD, Magnani B, Minelli G, Piali G and Sotera BM** (1998) The structural style of the Umbria-Marche fold and thrust belt. *Memorie della Società Geologica Italiana* **52**, 557–78.
- Barchi MR** (2010) The Neogene–Quaternary evolution of the Northern Apennines: crustal structure, style of deformation and seismicity. In *The Geology of Italy* (eds M Beltrando, A Peccerillo, M Mattei, S Conticelli, and C Dogliani). *Journal of the Virtual Explorer* **36**, paper 11. doi: [10.3809/jvirtex.2009.00220](https://doi.org/10.3809/jvirtex.2009.00220).
- Bartole R** (1995) The North–Tyrrhenian–Northern Apennines post-collisional system: constraints for a geodynamic model. *Terranova* **1**, 7–30.
- Basili R and Valensise G** (2001) Seismogenic sources from Geologic/Geophysical data: 31-Fano Ardizio, 32-Pesaro San Bartolo, 33-Rimini Offshore North, 35-Rimini, 36-Val Marecchia. In *Database of Potential Sources for Earthquakes Larger than M = 5.5 in Italy* (eds L Valensise and D Pantosti), p. 44. Rome: Annali di Geofisica.
- Batini R, Console R and Luongo G** (1985) Seismological study of Larderello–Travale geothermal area. *Geothermics* **14**, 255–72.
- Bell RE, McNeill LC, Bull JM, Henstock TJ, Collier REL and Leeder MR** (2009) Fault architecture, basin structure and evolution of the Gulf of Corinth Rift, central Greece. *Basin Research* **21**, 824–55. doi: [10.1111/j.1365-2117.2009.00401.x](https://doi.org/10.1111/j.1365-2117.2009.00401.x).
- Bemporad S, Conedera C, Dainelli P, Ercoli A and Facibeni P** (1986) Landsat imagery: a valuable tool for regional and structural geology. *Memorie della Società Geologica Italiana* **25**, 91–106.
- Bencini A, Duchi V and Rainero E** (1979) Indagine geochimica su alcune acque minerali della provincia di Firenze. *Rendiconti della Società Italiana di Mineralogia e Petrografia* **35**, 667–75.
- Benedetti L, Tapponier P, King GCP, Meyer B and Manighetti I** (2000) Growth folding and active thrusting in the Montello region, Veneto, northern Italy. *Journal of Geophysical Research: Solid Earth* **105**, 739–66. doi: [10.1029/1999JB900222](https://doi.org/10.1029/1999JB900222).
- Benvenuti M and DegliInnocenti D** (2001) The Pliocene deposits in the central-eastern Valdelsa basin (Florence, Italy) revised through facies analysis and unconformity-bounded stratigraphic units. *Rivista Italiana di Paleontologia e Stratigrafia* **107**, 265–86.
- Benvenuti M, del Conte S, Scarselli N and Dominici S** (2014) Hinterland basin development and infilling through tectonic and eustatic processes: latest Messinian–Gelasian Valdelsa Basin, Northern Apennines, Italy. *Basin Research* **26**, 387–402. doi: [10.1111/bre.12031](https://doi.org/10.1111/bre.12031).
- Benvenuti M, Dominici S and Rook L** (1995) Inquadramento stratigrafico-deposizionale delle faune a mammiferi villafranchiane (unita faunistica Triversa e Montopoli) del Valdarno Inferiore nella zona a Sud dell'Arno (Toscana). *Il Quaternario* **8**, 457–64.
- Bianco C, Brogi A, Caggianelli A, Giorgetti G, Liotta D and Meccheri M** (2015) HP-LT metamorphism in Elba Island: implications for the geodynamic evolution of the inner Northern Apennines (Italy). *Journal of Geodynamics* **91**, 13–25. doi: [10.1016/j.jog.2015.08.001](https://doi.org/10.1016/j.jog.2015.08.001).
- Boccaletti M, Coli M, Eva C, Ferrari G, Giglia G, Lazzarotto A, Merlanti F, Nicolich R, Papani G and Postpischl D** (1985) Considerations on the seismotectonics of the Northern Apennines. *Tectonophysics* **117**, 7–38. doi: [10.1016/0040-1951\(85\)90234-3](https://doi.org/10.1016/0040-1951(85)90234-3).
- Boccaletti M and Dainelli P** (1982) Il sistema regmatico neogenico-quaternario nell'area mediterranea: esempio di deformazione plastico-rigido post-collisionale. *Memorie della Società Geologica Italiana* **24**, 465–82.
- Bonini M, Boccaletti M, Moratti M and Sani F** (2001) Neogene crustal shortening and basin evolution in Tuscany (northern Apennines). *Ofioliti* **26**, 275–86.
- Bonini M and Moratti G** (1995) Evoluzione tettonica del bacino neogenico di Radicondoli–Volterra (Toscana meridionale). *Bollettino della Società Geologica Italiana* **114**, 549–76.
- Bonini M and Sani F** (2002) Extension and compression in the Northern Apennines (Italy) hinterland: evidence from the late Miocene–Pliocene Siena–Radicondoli basin and relations with basement structures. *Tectonics* **21**, doi: [10.1029/2001TC900024](https://doi.org/10.1029/2001TC900024).
- Bonini M, Sani F, Stucchi EM, Moratti G, Benvenuti M, Menanno G and Tanini C** (2014) Late Miocene shortening of the Northern Apennines back-arc. *Journal of Geodynamics* **74**, 1–31. doi: [10.1016/j.jog.2013.11.002](https://doi.org/10.1016/j.jog.2013.11.002).
- Boschi E, Guidoboni E, Ferrari G, Valensise G and Gasperini P** (1997) *CFTI, Catalogo dei Forti terremoti Italiani dal 461 a.c. al 1990*. Bologna: ING, Istituto Nazionale di Geofisica and SGA, Storia Geofisica Ambiente.
- Bossio A, Costantini A, Lazzarotto A, Liotta D and Mazzanti R** (1993b) Rassegna delle conoscenze sul neoautoctono toscano. *Memorie della Società Geologica Italiana* **49**, 17–98.
- Bossio A, Mazzei R, Salvatorini G and Sandrelli F** (1993a) Nuovi dati sui depositi Mio–Pliocenicici del settore meridionale del Bacino del Fiume Elsa. *Paleopelagos* **3**, 97–108.
- Bossio A, Mazzei R, Salvatorini G and Sandrelli F** (2002) Geologia dell'area compresa tra Siena e Poggibonsi (Bacino del Casino). *Atti della Società Toscana di Scienze Naturali Memorie* **107**, 69–75.
- Braun T, Caciagli M, Carapezza ML, Famiani D, Gattuso A, Lisi A, Marchetti A, Mele G, Pagliuca NM, Ranaldi M and Sortino F** (2018a) The seismic sequence of 30th May–9th June 2016 in the geothermal site of Torre Alfina (central Italy) and related variations in soil gas emissions. *Journal of Volcanology and Geothermal Research* **359**, 21–36. doi: [10.1016/j.jvolgeores.2018.06.005](https://doi.org/10.1016/j.jvolgeores.2018.06.005).
- Braun T, Cesca S, Kühn D, Martirosian-Janssen A and Dahm T** (2018b) Anthropogenic seismicity in Italy and its relation to tectonics: state of the art and perspectives. *Anthropocene* **21**, 80–94. doi: [10.1016/j.ancene.2018.02.001S](https://doi.org/10.1016/j.ancene.2018.02.001S).
- Brogi A** (2004) Faults linkage, damage rocks and hydrothermal fluid circulation: tectonic interpretation of the Rapolano Terme travertines (southern Tuscany, Italy) in the context of Northern Apennines Neogene–Quaternary extension. *Eclogae Geologicae Helvetiae* **97**, 307–20. doi: [10.1007/s00015-004-1134-5](https://doi.org/10.1007/s00015-004-1134-5).
- Brogi A** (2006) Neogene extension in the Northern Apennines (Italy): insights from the southern part of the Mt. Amiata geothermal area. *Geodinamica Acta* **19**, 33–50. doi: [10.3166/ga.19.33-50](https://doi.org/10.3166/ga.19.33-50).
- Brogi A** (2008) Kinematics and geometry of Miocene low-angle detachments and exhumation of the metamorphic units in the hinterland of the Northern Apennines (Italy). *Journal of Structural Geology* **30**, 2–20.
- Brogi A** (2011) Bowl-shaped basin related to low-angle detachment during continental extension: the case of the controversial Neogene Siena Basin (central Italy, Northern Apennines). *Tectonophysics* **499**, 54–76.
- Brogi A** (2020) Late evolution of the inner Northern Apennines from the structure of the Monti del Chianti–Monte Cetona ridge (Tuscany, Italy). *Journal of Structural Geology* **141**, 104205. doi: [10.1016/j.jsg.2020.104205](https://doi.org/10.1016/j.jsg.2020.104205).
- Brogi A, Capezzuoli E, Aqué R, Branca M and Voltaggio M** (2010) Studying travertines for neotectonics investigations: Middle–Late Pleistocene syn-tectonic travertine deposition at Serre di Rapolano (Northern Apennines, Italy). *International Journal of Earth Sciences* **99**, 1383–98. doi: [10.1007/s00531-009-0456-y](https://doi.org/10.1007/s00531-009-0456-y).
- Brogi A, Capezzuoli E, Kele S, Baykara MO and Shen C-C** (2017) Key travertine tectofacies for neotectonics and palaeoseismicity reconstruction: effects of hydrothermal overpressured fluid injection. *Journal of the Geological Society* **174**, 679–99. doi: [10.1144/jgs2016-124](https://doi.org/10.1144/jgs2016-124).
- Brogi A, Capezzuoli E, Martini I, Picozzi M and Sandrelli F** (2014) Late Quaternary tectonics in the inner Northern Apennines (Siena basin, southern Tuscany, Italy) and their seismotectonic implication. *Journal of Geodynamics* **76**, 25–45.
- Brogi A and Fabbri L** (2009) Extensional and strike-slip tectonics across the Monte Amiata–Monte Cetona transect (Northern Apennines, Italy) and seismotectonic implications. *Tectonophysics* **476**, 195–209. doi: [10.1016/j.tecto.2009.02.020](https://doi.org/10.1016/j.tecto.2009.02.020).

- Brogi A, Fidolini F and Liotta D** (2013) Tectonic and sedimentary evolution of the Upper Valdarno Basin: new insights from the lacustrine S. Barbara Basin. *Italian Journal of Geosciences* **132**, 81–97. doi: [10.3301/IJG.2012.08](https://doi.org/10.3301/IJG.2012.08).
- Brogi A and Giorgetti G** (2012) Tectono-metamorphic evolution of the siliciclastic units in the Middle Tuscan Range (inner Northern Apennines): Mg-carpholite bearing quartz veins related to syn-metamorphic syn-orogenic foliation. *Tectonophysics* **526–529**, 167–84. doi: [10.1016/j.tecto.2011.09.015](https://doi.org/10.1016/j.tecto.2011.09.015).
- Brogi A, Lazzarotto A, Liotta D and Ranalli G** (2005) Crustal structures in the geothermal areas of southern Tuscany (Italy): insights from the CROP 18 deep seismic reflection lines. *Journal of Volcanology and Geothermal Research* **148**, 60–80. doi: [10.1016/j.jvolgeores.2005.03.014](https://doi.org/10.1016/j.jvolgeores.2005.03.014).
- Brogi A and Liotta D** (2008) Highly extended terrains, lateral segmentation of the substratum, and basin development: the middle-late Miocene Radicondoli Basin (inner Northern Apennines, Italy). *Tectonics* **27**, TC5002. doi: [10.1029/2007TC002188](https://doi.org/10.1029/2007TC002188).
- Buonasorte G, Cataldi R, Ceccarelli A, Costantini A, D'offizi S, Lazzarotto A, Ridolfi A, Baldi P, Barelli A, Bertini G and Bertrami R** (1988) Ricerca ed esplorazione nell'area geotermica di Torre Alfina (Lazio - Umbria). *Bollettino della Società Geologica Italiana* **107**, 265–37.
- Buonasorte G, Fiordelisi A and Rossi U** (1987) Tectonic structures and geometric setting of the Vulsini Volcanic Complex. *Periodico di Mineralogia* **56**, 123–6.
- Buonasorte G, Pandeli F and Fiordelisi A** (1991) The Alfina 15 well: deep geological data from Northern Latium (Torre Alfina geothermal area). *Bollettino della Società Geologica Italiana* **110**, 823–31.
- Burrato P, Vannoli P, Fracassi U, Basili R and Valensise G** (2012) Is blind faulting truly invisible? Tectonic-controlled drainage evolution in the epicentral area of the May 2012, Emilia-Romagna earthquake sequence (northern Italy). *Annals of Geophysics*. doi: [10.4401/ag-6182](https://doi.org/10.4401/ag-6182).
- Calamai A, Cataldi R, Squarci P and Taffi L** (1970) Geology, geophysics and hydrogeology of the Monte Amiata geothermal field. *Geothermics* **1**, 1–9.
- Camassi R, Castelli V, Molin D, Bernardini F, Caracciolo CH, Ercolani E and Postpischl L** (2011) *Materiali per un catalogo dei terremoti italiani: eventi sconosciuti, rivalutati o riscoperti*, SN 96, ISSN 1590-2595. Retrieved from <http://hdl.handle.net/2122/7387>.
- Cameli GM, Dini I and Liotta D** (1993) Upper crustal structure of the Larderello geothermal field as a feature of post-collisional extensional tectonics (Southern Tuscany, Italy). *Tectonophysics* **224**, 413–23. doi: [10.1016/0040-1951\(93\)90041-H](https://doi.org/10.1016/0040-1951(93)90041-H).
- Canuti P, Morini D and Tacconi P** (1975) Studi di Geomorfologia Applicata, III) Analisi geomorfica quantitativa del bacino del Fiume Elsa (affluente del Fiume Arno). *Bollettino della Società Geologica Italiana* **94**, 443–63.
- Canuti P, Pranzini G and Sestini G** (1966) Provenienza ed ambiente di sedimentazione dei ciottolami del Pliocene di San Casciano (Firenze). *Memorie della Società Geologica Italiana* **5**, 340–64.
- Capezzuoli E., Foresi LM, Salvatorini G and Sandrelli F** (2005) New data on the Middle Pliocene sedimentation in the southern Valdelsa basin (Siena, Italy). *Bollettino della Società Geologica Italiana* **4**, 95–103.
- Capezzuoli E, Priori S, Costantini EAC and Sandrelli F** (2009) Stratigraphic and paleopedological aspects from the Middle Pleistocene continental deposits of the southern Valdelsa Basin. *Bollettino della Società Geologica Italiana* **128**, 395–402. doi: [10.3301/IJG.2009.128.2.395](https://doi.org/10.3301/IJG.2009.128.2.395).
- Carmignani L, Decandia FA, Disperati PL, Lazzarotto A, Liotta D and Meccheri M** (1994) Tertiary extensional tectonics in Tuscany (Northern Apennines Italy). *Tectonophysics* **238**, 295–315.
- Celati R, Grassi S and Calore C** (1990) Overflow thermal springs of Tuscany (Italy). *Journal of Hydrology* **118**, 191–207. doi: [10.1016/0022-1694\(90\)90258-Y](https://doi.org/10.1016/0022-1694(90)90258-Y).
- Chiarabba C, Jovane L and Stefano RD** (2005) A new view of the Italian seismicity using 20 years of instrumental recordings. *Tectonophysics* **395**, 251–68.
- Cioppi E** (1995) *18 Maggio 1895. Storia di un terremoto fiorentino*. Florence: Osservatorio Ximeniano, 305 pp.
- Collettini C, Paola ND, Holdsworth RE and Barchi MR** (2006) The development and behaviour of low-angle normal faults during Cenozoic asymmetric extension in the Northern Apennines, Italy. *Journal of Structural Geology* **28**, 333–52.
- Console R, Murru M and Alessandrini B** (1993) Foreshock statistics and their possible relationships to earthquake prediction in the Italian region. *Bulletin of the Seismological Society of America* **83**, 1248–63.
- Console R and Rosini R** (1998) Non-double-couple microearthquakes in the geothermal field of Larderello, central Italy. *Tectonophysics* **289**, 203–20.
- Dallmeyer RD and Liotta D** (1998) Extension, uplift of rocks and cooling ages in thinned crustal provinces: the Larderello geothermal area (inner Northern Apennines, Italy). *Geological Magazine* **135**, 193–202.
- De Luca G, Scarpa R, Filippi L, Gorini A, Marcucci S, Marsan P, Milana G and Zambonelli E** (1999) A detailed analysis of two seismic sequences in Abruzzo, Central Apennines. *Journal of Seismology* **2**, 1–21.
- Decandia FA, Lazzarotto A and Liotta D** (1993) La 'Serie ridotta' nel quadro dell'evoluzione geologica della Toscana meridionale. *Memorie della Società Geologica Italiana* **49**, 181–90.
- Della Vedova R, Bellani S, Pellis G and Squarci P** (2001) Deep temperatures and surface heat flow distribution. In *Anatomy of an Orogen: the Apennines and Adjacent Mediterranean Basins* (eds GB Vai and IP Martini), pp. 151–64. Dordrecht: Kluwer Academic Publishers.
- Di Bucci D and Mazzoli S** (2002) Active tectonics of the Northern Apennines and Adria geodynamics: new data and a discussion. *Journal of Geodynamics* **34**, 687–707.
- Di Bucci D, Ravaglia A, Seno S, Toscani G, Fracassi U and Valensise G** (2006) Seismotectonics of the Southern Apennines and Adriatic foreland: insights on active regional E–W shear zones from analogue modeling. *Tectonics* **25**, TC4015. doi: [10.1029/2005TC001898](https://doi.org/10.1029/2005TC001898).
- Dini A, Mazzarini F, Musumeci G and Rocchi S** (2008) Multiple hydrofracturing by boron-rich fluids in the Late Miocene contact aureole of eastern Elba Island (Tuscany, Italy). *Terra Nova* **20**, 318–26. doi: [10.1111/j.1365-3121.2008.00823.x](https://doi.org/10.1111/j.1365-3121.2008.00823.x).
- Doğan B and Karaka A** (2013) Geometry of co-seismic surface ruptures and tectonic meaning of the 23 October 2011 Mw 7.1 Van earthquake (East Anatolian Region, Turkey). *Journal of Structural Geology* **46**, 99–114. doi: [10.1016/j.jsg.2012.10.001](https://doi.org/10.1016/j.jsg.2012.10.001).
- Dogliani C** (1991) A proposal of kinematic modelling for W-dipping subductions-Possible applications to the Tyrrhenian-Apennines system. *Terranova* **3**, 423–34.
- Faenza L and Pierdominici S** (2007) Statistical occurrence analysis and spatio-temporal distribution of earthquakes in the Apennines (Italy). *Tectonophysics* **439**, 13–31.
- Farina F, Dini A, Innocenti F and Rocchi S** (2010) Rapid incremental assembly of the Monte Capanne pluton (Elba Island, Tuscany) by downward stacking of magma sheets. *Geological Society of America Bulletin* **122**, 9–10. doi: [10.1130/B30112.1](https://doi.org/10.1130/B30112.1).
- Fazzini P and Gelmini R** (1982) Tettonica trasversale nell'Appennino Settentrionale. *Memorie della Società Geologica Italiana* **24**, 299–309.
- Fazzuoli M, Garzonio CA and Vannocci P** (1983) Considerazioni sui caratteri strutturali e morfologici della parte settentrionale della dorsale medio-Toscana, nell'area di San Gimignano (Siena). *Memorie della Società Geologica Italiana* **25**, 165–83.
- Finetti IR** (2006) Basic regional crustal setting and superimposed local pluton intrusion related tectonics in the Larderello-Monte Amiata geothermal province, from integrated CROP seismic data. *Bollettino della Società Geologica Italiana* **125**, 117–46.
- Finetti IR, Boccaletti M, Bonini M, Ben AD, Geletti R, Pipan M and Sani F** (2001) Crustal section based on CROP seismic data across the North Tyrrhenian-Northern Apennines-Adriatic Sea. *Tectonophysics* **343**, 135–63.
- Foresi LM, Bambini AM, Mazzei R, Piccinelli B and Sandrelli F** (2003) La base dell'arenaria di Ponsano nella sua area tipo e nella zona di Casole d'Elsa (Toscana). *Atti della Società Toscana di Scienze Naturali* **10**.
- Galadini F and Galli P** (2000) Active tectonics in the Central Apennines (Italy): input data for seismic hazard assessment. *Natural Hazards* **22**, 225–70.
- Ghelardoni R** (1965) Osservazioni sulla tettonica trasversale dell'Appennino Settentrionale. *Bollettino della Società Geologica Italiana* **84**, 277–90.
- Gola G, Bertini G, Bonini M, Botteghi S, Brogi A, De Franco R, Dini A, Donato A, Gianelli G, Liotta D and Manzella A** (2017) Data integration

- and conceptual modelling of the Larderello geothermal area, Italy. *Energy Procedia* **125**, 300–9. doi: [10.1016/j.egypro.2017.08.201](https://doi.org/10.1016/j.egypro.2017.08.201).
- Gualtieri L, de Franco R and Mazzotti A** (1998) A velocity model along the CROP 03 profile derived from expanding spread experiments. *Memorie della Società Geologica Italiana* **52**, 139–52.
- Guidoboni E and Ferrari G** (1995) Historical cities and earthquakes: Florence during the last nine centuries and evaluations of seismic hazard. *Annali di Geofisica* **38**, 617–47.
- Hancock PL, Chalmers RML, Altunel E and Çakir Z** (1999) Travertines: using travertines in active fault studies. *Journal of Structural Geology* **21**, 903–16.
- Hauksson E, Jones L, Davis TL, Hutton LK, Williams P, Bent AL, Brady AG, Reasenber P, Michael AJ, Yerkes RF and Etheredge E** (1988) The 1987 Whittier Narrows Earthquake in the Los Angeles Metropolitan Area, California. *Science* **239**, 1409. doi: [10.1126/science.239.4846.1409](https://doi.org/10.1126/science.239.4846.1409).
- Hayes GP, Briggs RW, Sladen A, Fielding EJ, Prentice C, Hudnut K, Mann P, Taylor FW, Crone AJ, Gold R and Ito T** (2010) Complex rupture during the 12 January 2010 Haiti earthquake. *Nature Geoscience* **3**, 800–5. doi: [10.1038/ngeo977](https://doi.org/10.1038/ngeo977).
- Jolivet L, Dubois R, Fournier M, Goffe B, Michard A and Jourdan C** (1990) Ductile extension in alpine Corsica. *Geology* **18**, 1007–10.
- Latorre D, Mirabella F, Chiaraluca L, Trippetta F and Lomax A** (2016) Assessment of earthquake locations in 3-D deterministic velocity models: a case study from the Alototiberina Near Fault Observatory (Italy): event locations in deterministic models. *Journal of Geophysical Research: Solid Earth* **121**, 8113–35. doi: [10.1002/2016JB013170](https://doi.org/10.1002/2016JB013170).
- Lavecchia G** (1988) The Tyrrhenian-Apennines system: structural setting and seismotectogenesis. *Tectonophysics* **147**, 263–96.
- Lazzarotto A and Mazzanti R** (1978) Geologia dell'alta Val di Cecina. *Bollettino della Società Geologica Italiana* **95**, 1365–487.
- Lazzarotto A and Sandrelli F** (1977) Stratigrafia ed assetto tettonico delle formazioni neogeniche nel bacino del Casino (Siena). *Bollettino del Servizio Geologico d'Italia* **96**, 747–62.
- Lettis WR, Wells DL and Baldwin JN** (1997) Empirical observations regarding reverse earthquakes, blind thrust faults, and Quaternary deformation: are blind thrust faults truly blind? *Bulletin of the Seismological Society of America* **87**, 1171–98.
- Li YG, De Pascale GP, Quigley MC and Gravelly DM** (2014) Fault damage zones of the M7.1 Darfield and M6.3 Christchurch earthquakes characterized by fault-zone trapped waves. *Tectonophysics* **31**, 618:79–101.
- Liotta D** (1991) The Arbia-Val Marecchia line, Northern Apennines. *Eclogae Geologicae Helveticae* **84**, 413–30.
- Liotta D and Brogi A** (2020) Pliocene-Quaternary fault kinematics in the Larderello geothermal area (Italy): insights for the interpretation of the present stress field. *Geothermics* **83**, 101714. doi: [10.1016/j.geothermics.2019.101714](https://doi.org/10.1016/j.geothermics.2019.101714).
- Liotta D, Brogi A, Meccheri M, Dini A, Bianco C and Ruggieri G** (2015) Coexistence of low-angle normal and high-angle strike- to oblique-slip faults during Late Miocene mineralization in eastern Elba Island (Italy). *Tectonophysics* **660**, 17–34.
- Liotta D, Cernobori L and Nicolici L** (1998) Restricted rifting and its coexistence with compressional structures: results from the CROP 3 traverse (Northern Apennines, Italy). *Terra Nova* **10**, 16–20. doi: [10.1046/j.1365-3121.1998.00157.x](https://doi.org/10.1046/j.1365-3121.1998.00157.x).
- Lisi A, Marchetti A, Frepoli A, Pagliuca NM, Mele G, Carapezza ML, Caciagli M, Famiani D, Gattuso A and Braun T** (2019) Microseismicity analysis in the geothermal area of Torre Alfina, Central Italy. *Journal of Seismology* **23**, 1279–98. doi: [10.1007/s10950-019-09865-8](https://doi.org/10.1007/s10950-019-09865-8).
- Locati M, Camassi RD, Rovida AN, Ercolani E, Bernardini FM, Castelli V, Caracciolo CH, Tertulliani A, Rossi A, Azzaro R and D'Amico S** (2021) Database Macrosismico Italiano (DBMI15), versione 3.0. Istituto Nazionale di Geofisica e Vulcanologia (INGV) Rome. doi: [10.13127/DBMI/DBMI15.2](https://doi.org/10.13127/DBMI/DBMI15.2).
- Lotti B** (1900) Foglio 113 'S.Casciano in Val di Pesa'. *Carta Geologica d'Italia, scala 1:100.000*. Rome: Regio Servizio Geologico d'Italia.
- Lotti B, Fossen P and Canavari M** (1908) Foglio 106 'Firenze'. *Carta Geologica d'Italia, scala 1:100.000*. Rome: Regio Servizio Geologico d'Italia.
- Mariani M and Prato R** (1988) I bacini neogenici costieri del margine tirrenico: approccio sismostratigrafico. *Memorie della Società Geologica Italiana* **41**, 519–31.
- Marrett R and Allmendinger RW** (1990) Kinematic analysis of fault-slip data. *Journal of Structural Geology* **12**, 973–86.
- Martini I, Ambrosetti E, Brogi A, Aldinucci M, Zwaan F and Sandrelli F** (2021) Polyphase extensional basins: interplay between tectonics and sedimentation in the Neogene Siena-Radicofani Basin (Northern Apennines, Italy). *International Journal of Earth Sciences* **110**, 1729–51. doi: [10.1007/s00531-021-02038-4](https://doi.org/10.1007/s00531-021-02038-4).
- Martini IP and Sagri M** (1993) Tectono-sedimentary characteristics of late Miocene-Quaternary extensional basins of the Northern Apennines, Italy. *Earth Science Reviews* **34**, 197–233. doi: [10.1016/0012-8252\(93\)90034-5](https://doi.org/10.1016/0012-8252(93)90034-5).
- Mazzanti R** (1966) Geologia della zona di Pomarance-Larderello (Prov. di Pisa). *Memorie della Società Geologica Italiana* **5**, 105–38.
- Merla G and Bortolotti V** (1967) *Note illustrative della Carta Geologica d'Italia in scala 1:100.000. Foglio n°113 Castelfiorentino (II Edizione)*. Rome: Servizio Geologico d'Italia.
- Merla G, Bortolotti V and Passerini P** (1967) *Note illustrative della Carta Geologica d'Italia in scala 1:100.000. Foglio n°106 Firenze (II Edizione)*. Rome: Servizio Geologico d'Italia.
- Michele M, Chiaraluca L, di Stefano R and Waldhauser F** (2020) Fine-scale structure of the 2016–2017 Central Italy seismic sequence from data recorded at the Italian National Network. *Journal of Geophysical Research: Solid Earth* **125**. doi: [10.1029/2019JB018440](https://doi.org/10.1029/2019JB018440).
- Minissale A** (2004) Origin, transport and discharge of CO₂ in central Italy. *Earth Science Reviews* **66**, 89–141.
- Mirabella F, Barchi MR, Lupattelli A, Stucchi E and Ciaccio MG** (2008) Insights on the seismogenic layer thickness from the upper crust structure of the Umbria-Marche Apennines (Central Italy). *Tectonics* **27**, TC1010. doi: [10.1029/2007TC002134](https://doi.org/10.1029/2007TC002134).
- Molli G, Manighetti I, Bennett R, Malavieille J, Serpelloni E, Storti F, Giampietro T, Bigot A, Pinelli G, Giacomelli S, Lucca A, Angeli L and Porta A** (2021) Active fault systems in the Inner Northwest Apennines, Italy: a reappraisal one century after the 1920 Mw ~6.5 Fivizzano earthquake. *Geosciences* **11**, 139. doi: [10.3390/geosciences11030139](https://doi.org/10.3390/geosciences11030139).
- Molli G** (2008) Northern Apennine-Corsica orogenic system: an updated overview. In *Tectonic Aspects of the Alpine-Dinaride-Carpathian System* (eds S Siegesmund, B Fügenschuh and N Frotzheim), pp. 413–42. Geological Society of London, Special Publication no. 298. doi: [10.1144/SP298.19](https://doi.org/10.1144/SP298.19).
- Mongelli F and Zito G** (1991) Flusso di calore nella regione Toscana. *Studi Geologici Camerti, Vol. Spec.* 1991/1, 91–8.
- Negredo AM, Barba S, Carminati E, Sabadini R and Giunchi C** (1999) Contribution of numeric dynamic modelling to the understanding of the seismotectonic regime of the Northern Apennines. *Tectonophysics* **315**, 15–30.
- Nirta G, Vittori E, Blumetti AM, Di Manna P, Benvenuti M, Montanari D, Perini M, Fiera F, Moratti G, Baglione M and Piccardi L** (2021) Geomorphological and paleoseismological evidence of capable faulting in the Northern Apennines (Italy): insights into active tectonics and seismic hazard of the Lunigiana basin. *Geomorphology* **374**, 107486. doi: [10.1016/j.geomorph.2020.107486](https://doi.org/10.1016/j.geomorph.2020.107486).
- Pace B, Peruzza L, Lavecchia G and Boncio P** (2006) Layered seismogenic source model and probabilistic seismic-hazard analyses in central Italy. *Bulletin of the Seismological Society of America* **96**, 107–32.
- Pandeli E, Bertini G and Castellucci P** (1991) The tectonic wedges complex of the Larderello area (southern Tuscany – Italy). *Bollettino della Società Geologica Italiana* **110**, 621–9.
- Pascucci V, Martini IP, Sagri M and Sandrelli F** (2007) Effects of transverse structural lineaments on the Neogene-Quaternary basins of Tuscany (inner Northern Apennines, Italy). In *Sedimentary Processes, Environments and Basins: A Tribute to Peter Friend* (eds G Nichols, E Williams, and C Paola), pp. 155–182. International Association of Sedimentologists, Special Publication no. 38. Oxford: Blackwell Publishing.
- Pascucci V, Merlini S and Martini IP** (1999) Seismic stratigraphy of the Miocene–Pleistocene sedimentary basins of the Northern Tyrrhenian Sea and Western Tuscany (Italy). *Basin Research* **11**, 337–56.

- Pasini M and Sandrelli F** (1977) L'Arenaria di Ponsano nell'area a sud-est di Castellina Scalo (Siena). *Rivista Italiana di Paleontologia e Stratigrafia* **83**, 641–64.
- Patacca E, Sartori R and Scandone P** (1990) Tyrrhenian basin and Apenninic arcs: kinematic relations since late Tortonian times. *Memorie della Società Geologica Italiana* **45**, 425–51.
- Pasini M, Barchi MR, Federico C, Magnani MB and Minelli G** (2006) The crustal structure of the Northern Apennines (central Italy): and insight by the Crop03 seismic line. *American Journal of Science* **306**, 428–50. doi: [10.2475/06.2006.02](https://doi.org/10.2475/06.2006.02).
- Pera E, Mainprice D and Burlini L** (2003) Anisotropic seismic properties of the upper mantle beneath the Torre Alfina area (Northern Apennines, Central Italy). *Tectonophysics* **370**, 11–30.
- Piccardi L, Gaudemer Y, Tapponnier P and Boccaletti M** (1999) Active oblique extension in the central Apennines (Italy): evidence from the Fucino region. *Geophysical Journal International* **139**, 499–530. doi: [10.1046/j.1365-246x.1999.00955.x](https://doi.org/10.1046/j.1365-246x.1999.00955.x).
- Piccardi L, Vittori E, Blumetti AM, Comerci V, Di Manna P, Guerrieri L, Baglione M and D'Intinosante V** (2017) Mapping capable faulting hazard in a moderate-seismicity, high heat-flow environment: the Tuscia province (southern Tuscany-northern Latium, Italy). *Quaternary International* **451**, 11–36. doi: [10.1016/j.quaint.2017.07.018](https://doi.org/10.1016/j.quaint.2017.07.018).
- Pratt TL, Dolanz JF, Odum JK, Stephenson WJ, Williams RA and Templeton ME** (1998) Multiscale seismic imaging of active fault zones for hazard assessment: a case study of the Santa Monica fault zone, Los Angeles, California. *Geophysics* **63**, 479–89.
- Pucci S, Mirabella F, Pazzaglia F, Barchi MR, Melelli L, Tuccimei P *et al.*** (2014) Interaction between regional and local tectonic forcing along a complex Quaternary extensional basin: Upper Tiber Valley, Northern Apennines, Italy. *Quaternary Science Reviews* **102**, 111–32. doi: [10.1016/j.quascirev.2014.08.009](https://doi.org/10.1016/j.quascirev.2014.08.009).
- Ritz J-F, Baize S, Ferry M, Larroque C, Audin L, Delouis B and Mathot E** (2020) Surface rupture and shallow fault reactivation during the 2019 Mw 4.9 Le Teil earthquake, France. *Communications Earth & Environment* **1**, 10. doi: [10.1038/s43247-020-0012-z](https://doi.org/10.1038/s43247-020-0012-z).
- Rosenbaum G and Piana Agostinetti N** (2015) Crustal and upper mantle responses to lithospheric segmentation in the northern Apennines. *Tectonics* **34**, 648–61.
- Rossetti F, Faccenna C, Jolivet L, Funicello R, Tecce F and Brunet C** (1999) Syn- versus post-orogenic extension: the case study of Giglio Island (Northern Tyrrhenian Sea, Italy). *Tectonophysics* **304**, 73–92.
- Rossetti F, Faccenna C, Jolivet L, Goff B and Funicello R** (2002) Structural signature and exhumation P–T–t paths of the blueschist units exposed in the interior of the Northern Apennine chain, tectonic implications. *Bollettino della Società Geologica Italiana* **1**, 829–42.
- Rossetti F, Glodny J, Theye T and Maggi M** (2015) Pressure–temperature–deformation–time of the ductile Alpine shearing in Corsica: from orogenic construction to collapse. *Lithos* **218–219**, 99–116.
- Rovida AN, Locati M, Camassi RD, Lolli B and Gasperini P** (2016) *Catalogo parametrico dei terremoti italiani CPTI11* (Vol. <http://emidius.mi.ingv.it/CPTI>). Milan: Istituto Nazionale di Geofisica e Vulcanologia. doi: [10.6092/INGV.IT-CPTI11](https://doi.org/10.6092/INGV.IT-CPTI11).
- Selvaggi G and Amato A** (1992) Subcrustal earthquakes in the northern Apennines (Italy): evidence for a still active subduction? *Geophysical Research Letters* **19**, 2127–30.
- Shaw JH and Suppe J** (1994) Active faulting and growth folding in the eastern Santa Barbara Channel, California. *Geological Society of America Bulletin* **106**, 607–26. doi: [10.1130/0016-7606\(1994\)106<0607:AFAGFI>2.3.CO;2](https://doi.org/10.1130/0016-7606(1994)106<0607:AFAGFI>2.3.CO;2).
- Toscani G, Burrato P, Bucci DD, Seno S and Valensise G** (2009) Plio-Quaternary tectonic evolution of the Northern Apennines thrust fronts (Bologna-Ferrara section, Italy): seismotectonic implications. *Italian Journal of Geosciences* **128**, 605–13.
- Vai GB and Martini IP** (2001) *Anatomy of an Orogen: The Apennines and Adjacent Mediterranean Basins*. Dordrecht: Kluwer Academic Publishers.
- Valoroso L, Chiaraluce L, Di Stefano R and Monachesi G** (2017) Mixed-mode slip behavior of the Altotiberina low-angle normal fault system (Northern Apennines, Italy) through high-resolution earthquake locations and repeating events: seismic activity of low-angle ATF system. *Journal of Geophysical Research: Solid Earth* **122**, 10,220–40. doi: [10.1002/2017JB014607](https://doi.org/10.1002/2017JB014607).